Supplementary Information for the manuscript:

On the impact of competing intra- and intermolecular triplet-state quenching on photobleaching and photoswitching kinetics of organic fluorophores

Content

2. Details on chemical synthesis

1. Additional data

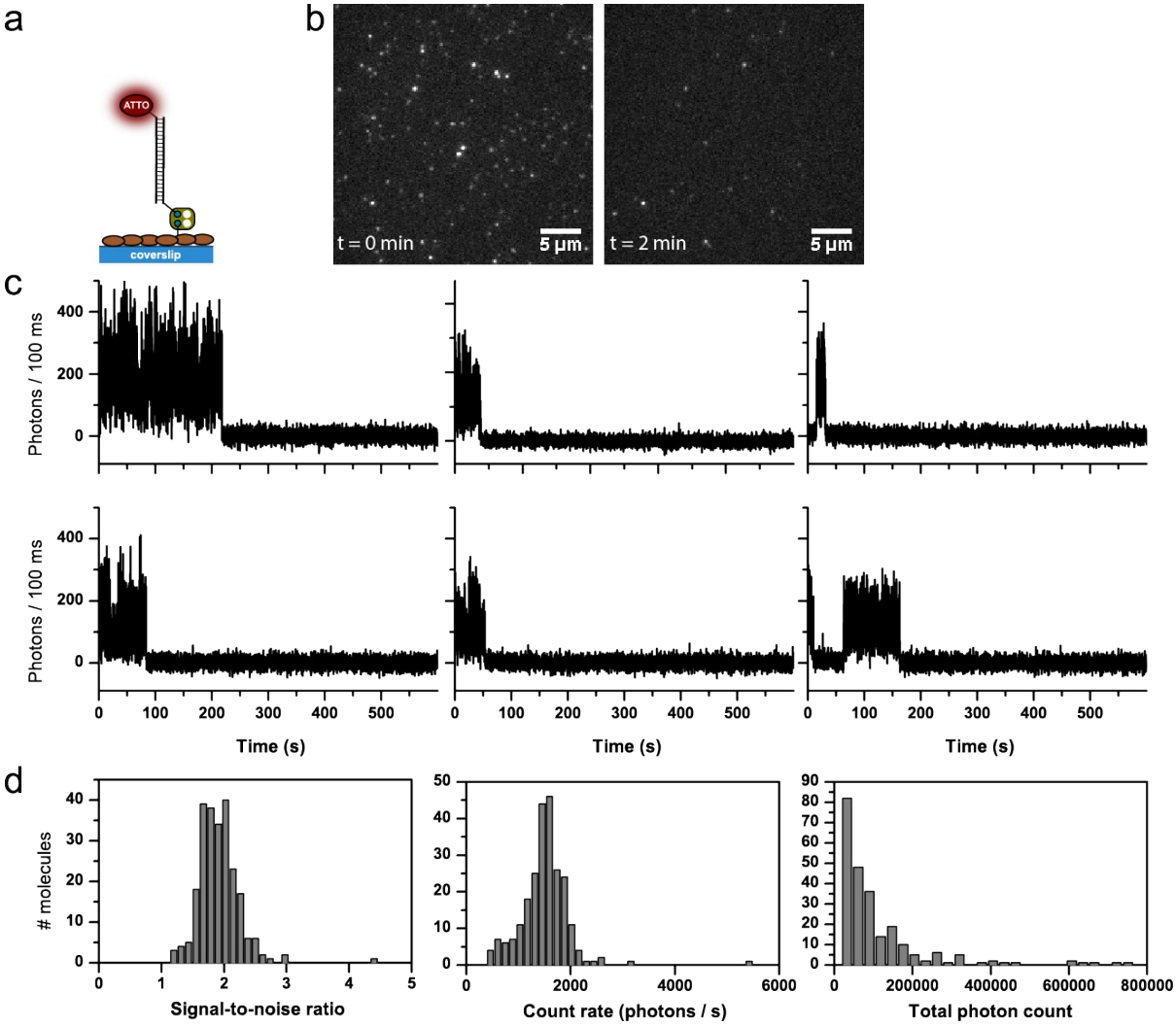

Figure S1: Detailed photophysical characterization of ATTO647N (GOX buffer, no photostabilizer in solution). a) Schematic representation of dye conjugation on DNA immobilized on a BSA/BSA-Biotin surface. b) TIRF images at different points in time, brightness and contrast 2848 to 35868 (AD counts). c) Representative time traces. d) Histograms of signal-to-noise ratio, count-rate and total photon count from individual time traces.

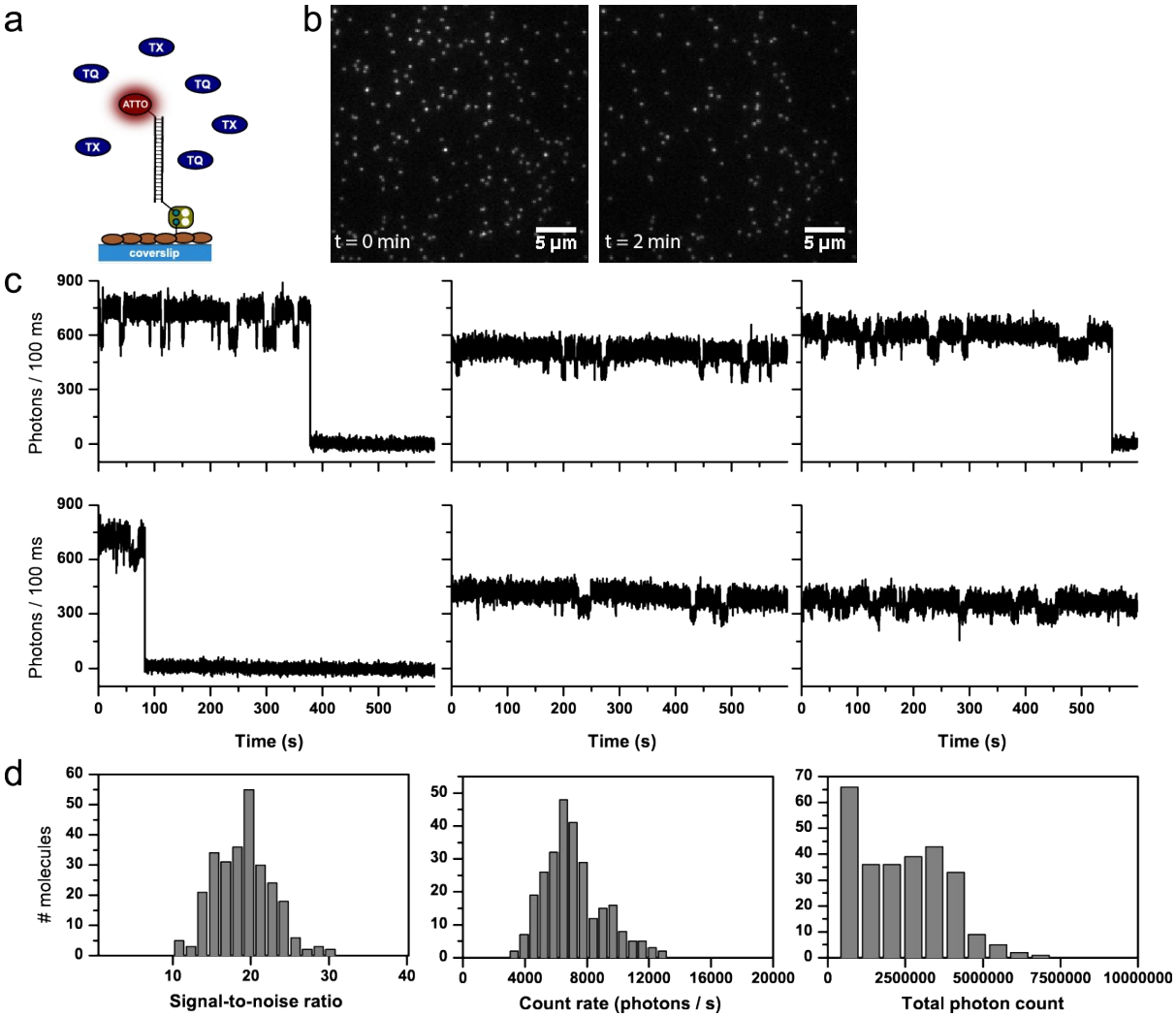

Figure S2: Detailed photophysical characterization of ATTO647N (buffer with 2 mM TX). a) Schematic representation of dye conjugation on DNA immobilized on a BSA/BSA-Biotin surface. **b) TIRF images at different points in time, brightness and contrast 3494 to 54418 (AD counts). c) Representative time traces. d) Histograms of signal-to-noise ratio, count-rate and total photon count from individual time traces.**

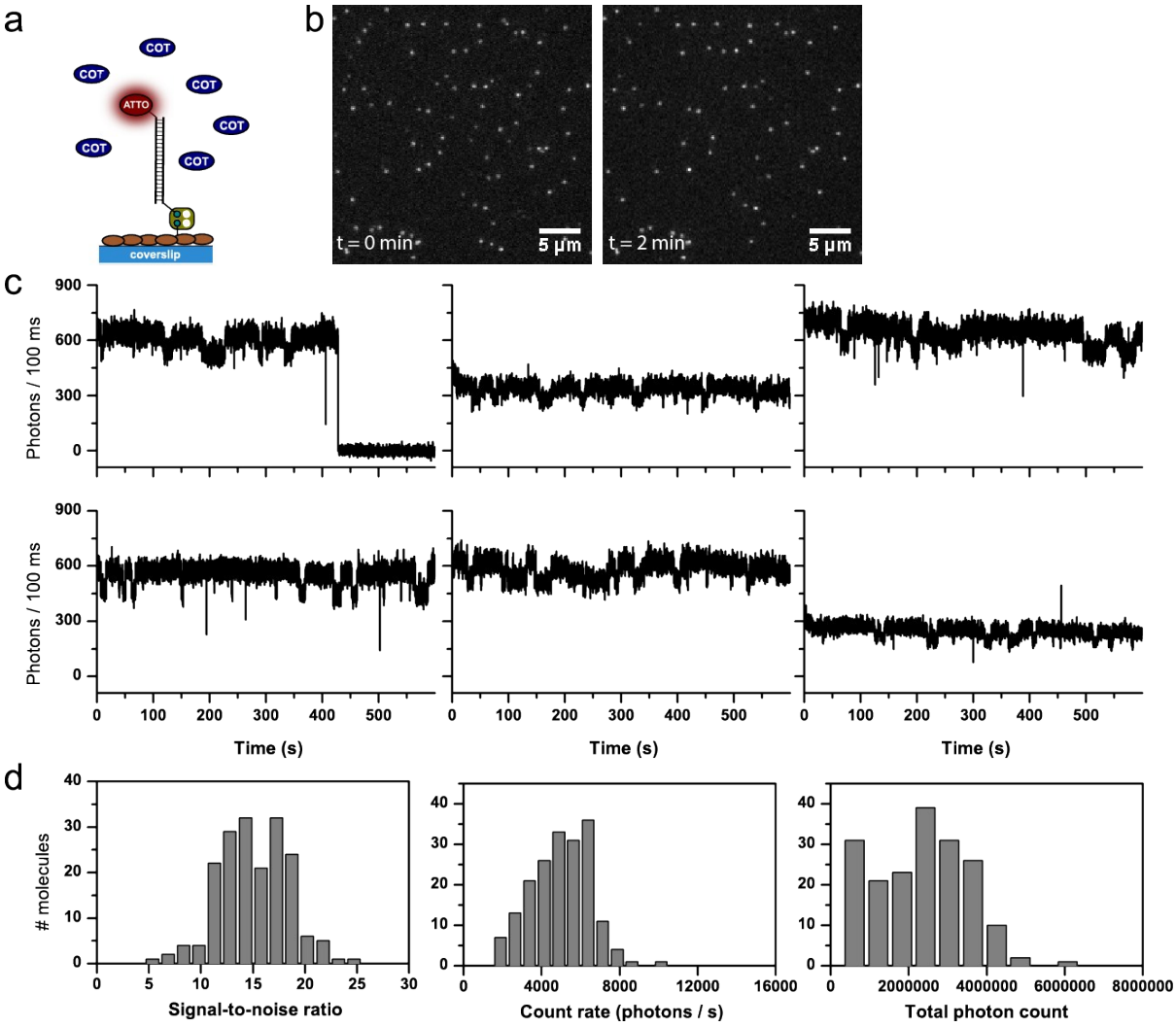

Figure S3: Detailed photophysical characterization of ATTO647N (**buffer with 2 mM COT**). a) Schematic representation of dye conjugation on DNA immobilized on a BSA/BSA-Biotin surface. b) TIRF images at different points in time, brightness and contrast 2394 to 16983 (AD counts). c) Representative time traces. d) Histograms of signal-to-noise ratio, count-rate and total photon count from individual time traces.

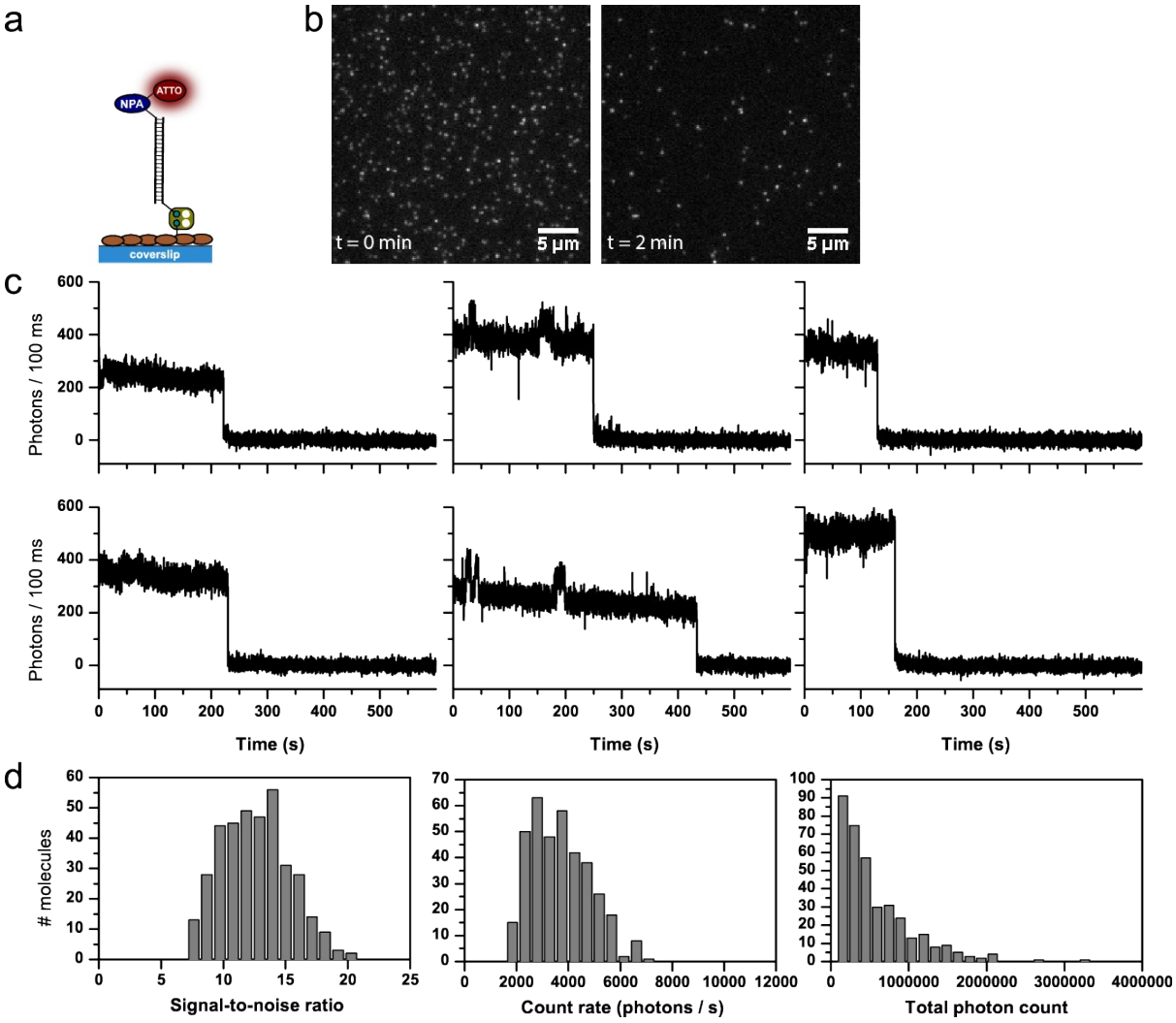

Figure S4: Detailed photophysical characterization of NPA-ATTO647N (GOX buffer, no photostabilizer in solution)**. a)** Schematic representation of dye conjugation on DNA immobilized on a BSA/BSA-Biotin surface. **b) TIRF images at different points in time, brightness and contrast 3037 to 24420 (AD counts). c) Representative time traces. d) Histograms of signal-to-noise ratio, count-rate and total photon count from individual time traces.**

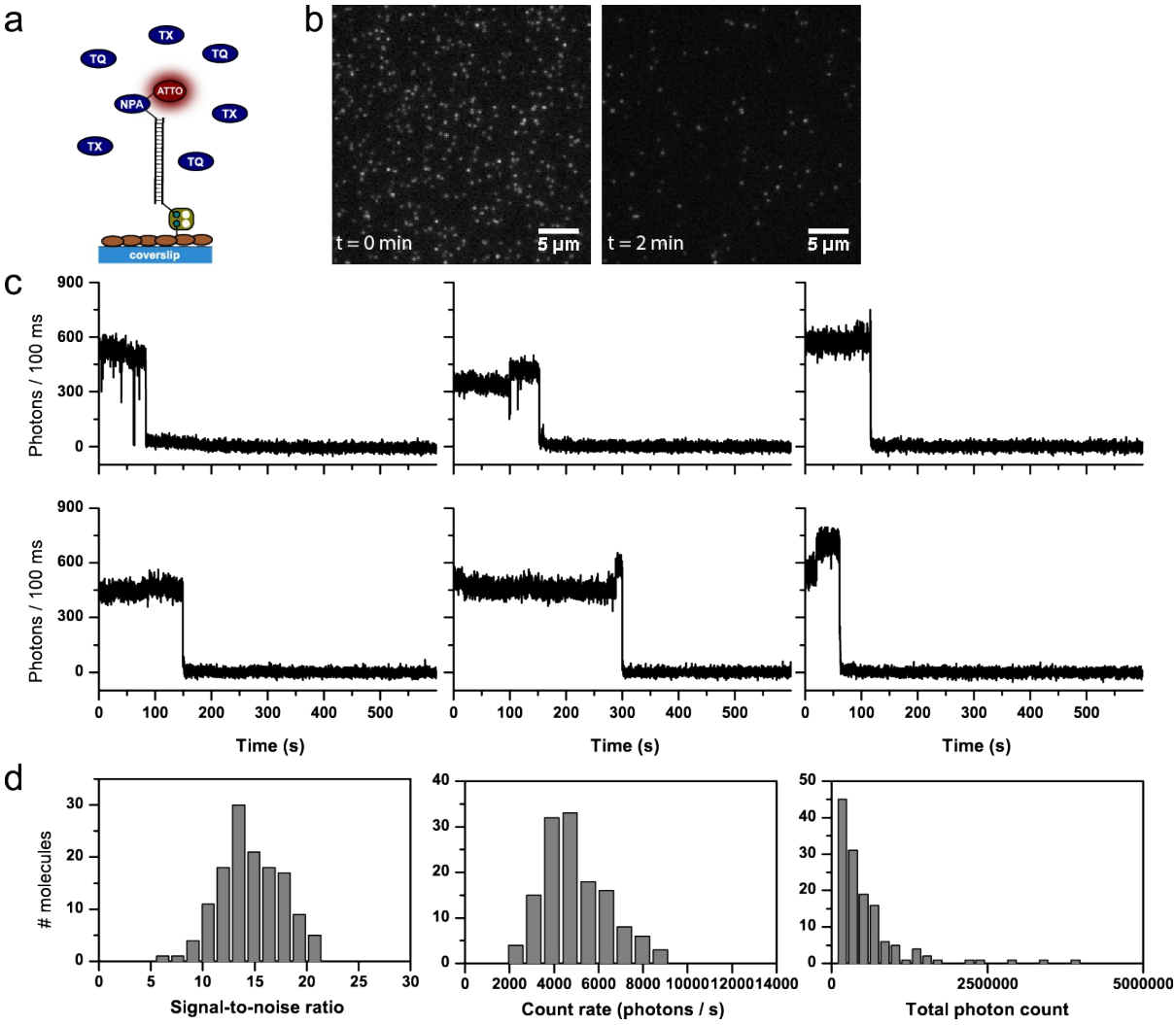

Figure S5: Detailed photophysical characterization of NPA-ATTO647N (buffer with 2 mM TX). a) Schematic representation of photostabilizer-dye conjugates on DNA immobilized on a BSA/BSA-Biotin surface. b) TIRF images at different points in time, brightness and contrast 3177 to 25515 (AD counts). c) Representative time traces. d) Histograms of signal-to-noise ratio, count-rate and total photon count from individual time traces.

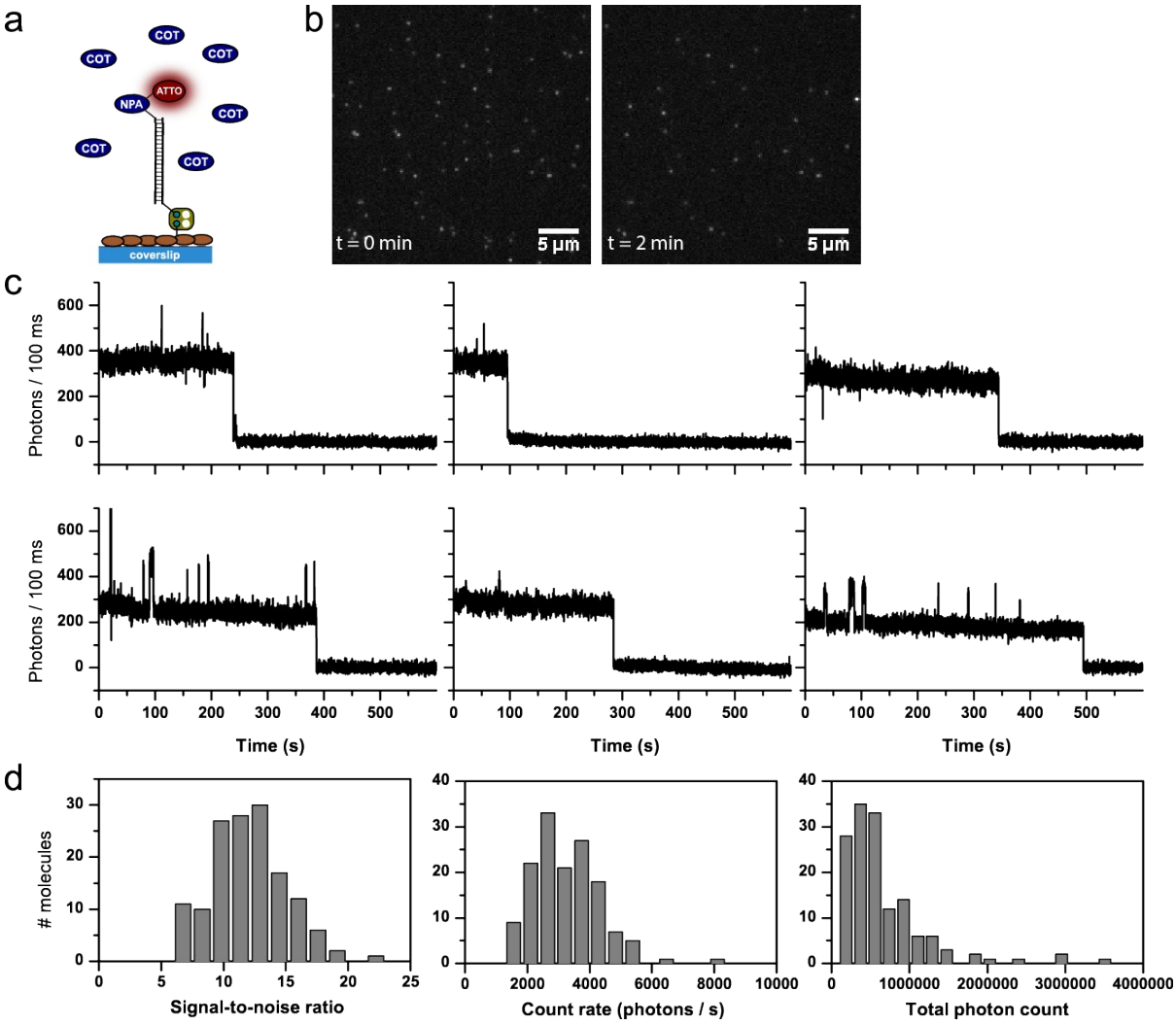

Figure S6: Detailed photophysical characterization of NPA-ATTO647N (buffer with 2 mM COT). a) Schematic representation of photostabilizer-dye conjugates on DNA immobilized on a BSA/BSA-Biotin surface. b) TIRF images at different points in time, brightness and contrast 2699 to 25823 (AD counts). c) Representative time traces. d) Histograms of signal-to-noise ratio, count-rate and total photon count from individual time traces.

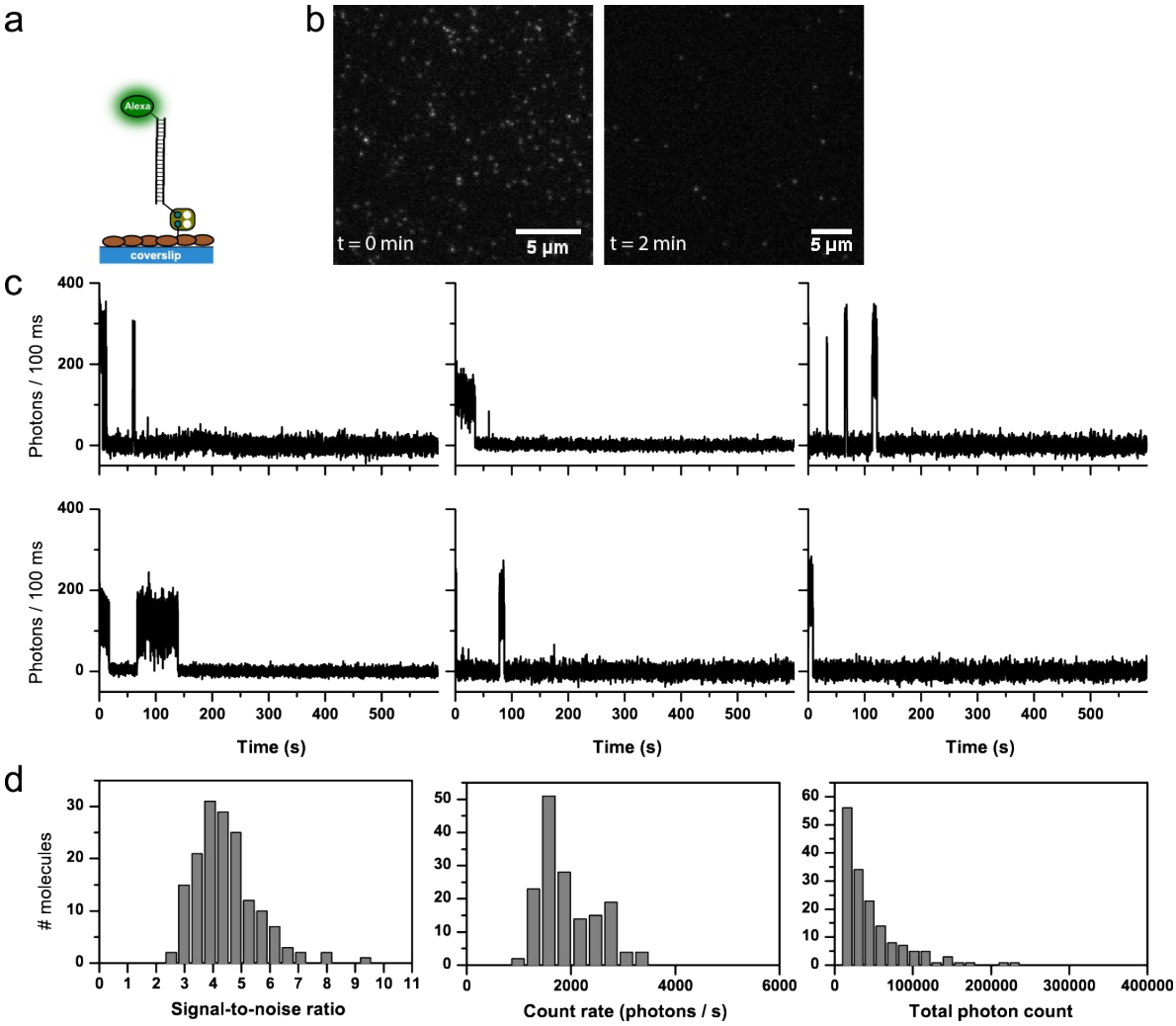

Figure S7: Detailed photophysical characterization of Alexa555 (GOX buffer, no photostabilizer in solution)**. a)** Schematic representation of dye conjugation on DNA immobilized on a BSA/BSA-Biotin surface. **b) TIRF images at different points in time, brightness and contrast 1876 to 14482 (AD counts). c) Representative time traces. d) Histograms of signal-to-noise ratio, count-rate and total photon count from individual time traces.**

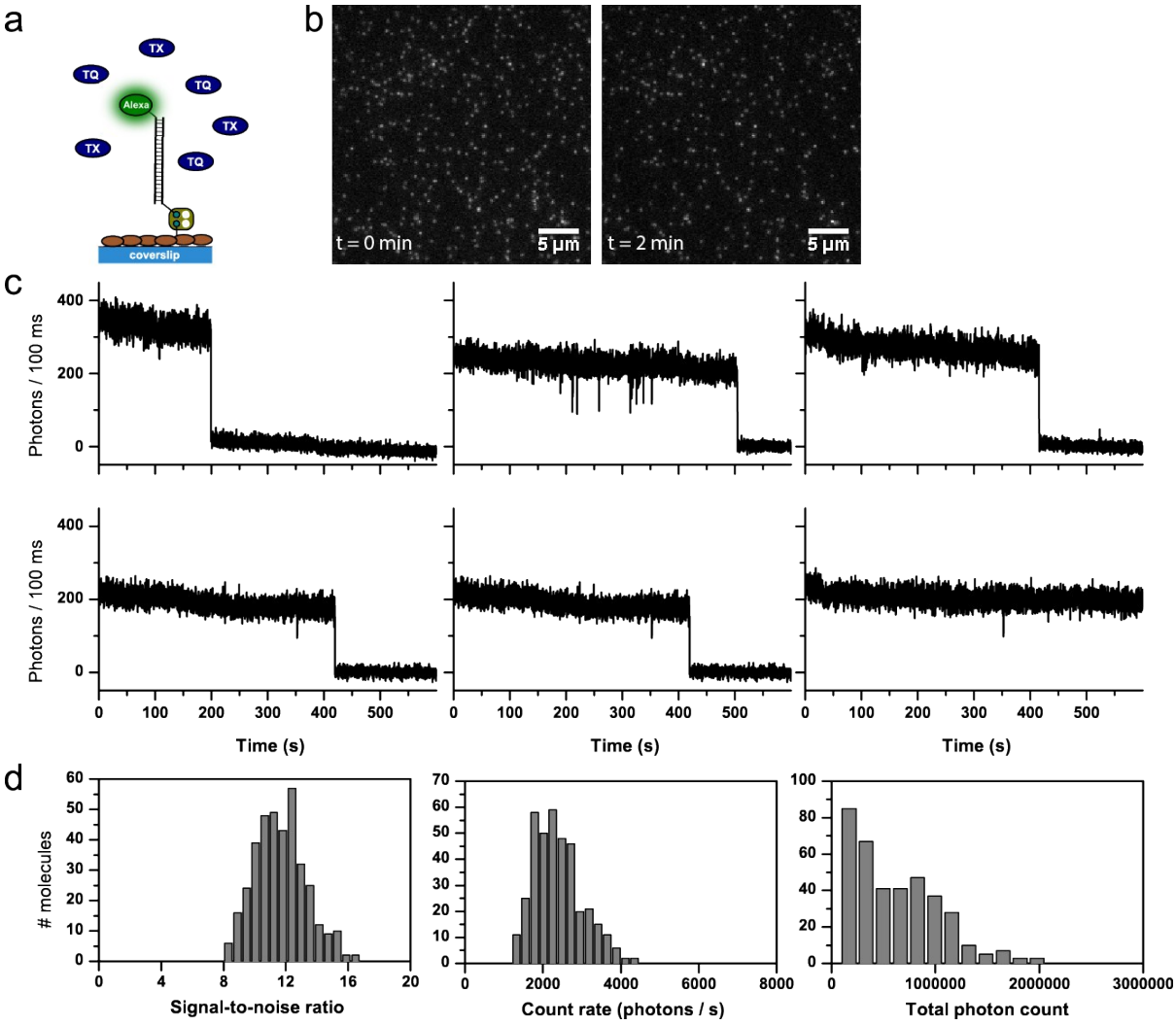

Figure S8: Detailed photophysical characterization of Alexa555 (buffer with 2 mM TX). a) Schematic representation of dye conjugation on DNA immobilized on a BSA/BSA-Biotin surface. b) TIRF images at different points in time, brightness and contrast 2083 to 16300 (AD counts). c) Representative time traces. d) Histograms of signal-to-noise ratio, count-rate and total photon count from individual time traces.

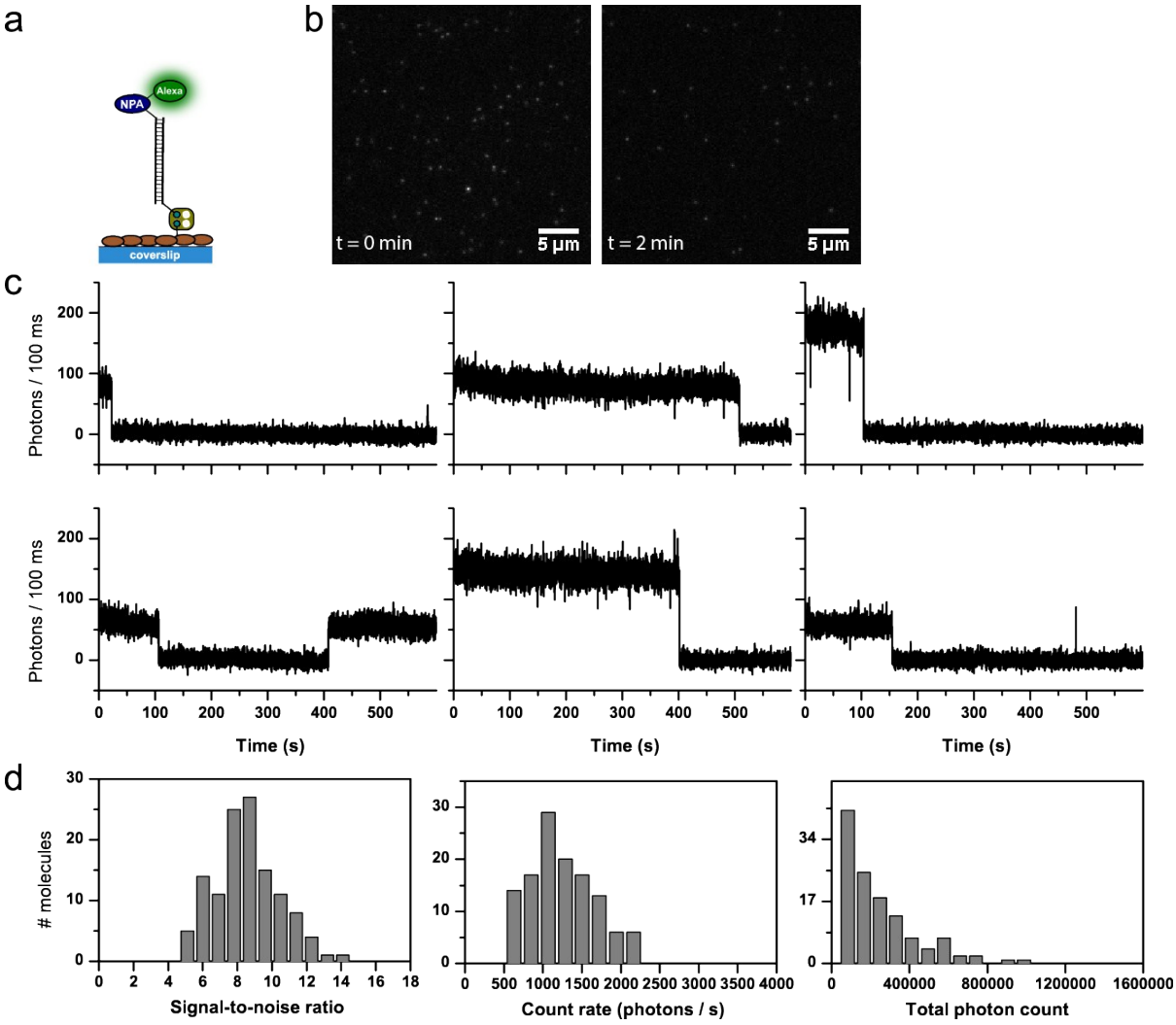

Figure S9: Detailed photophysical characterization of NPA-Alexa555 (GOX buffer, no photostabilizer in solution**). a) Schematic representation of photostabilizer-dye conjugates on DNA immobilized on a BSA/BSA-Biotin surface. b) TIRF images at different points in time, brightness and contrast 1904 to 19752 (AD counts). c) Representative time traces. d) Histograms of signal-to-noise ratio, count-rate and total photon count from individual time traces.**

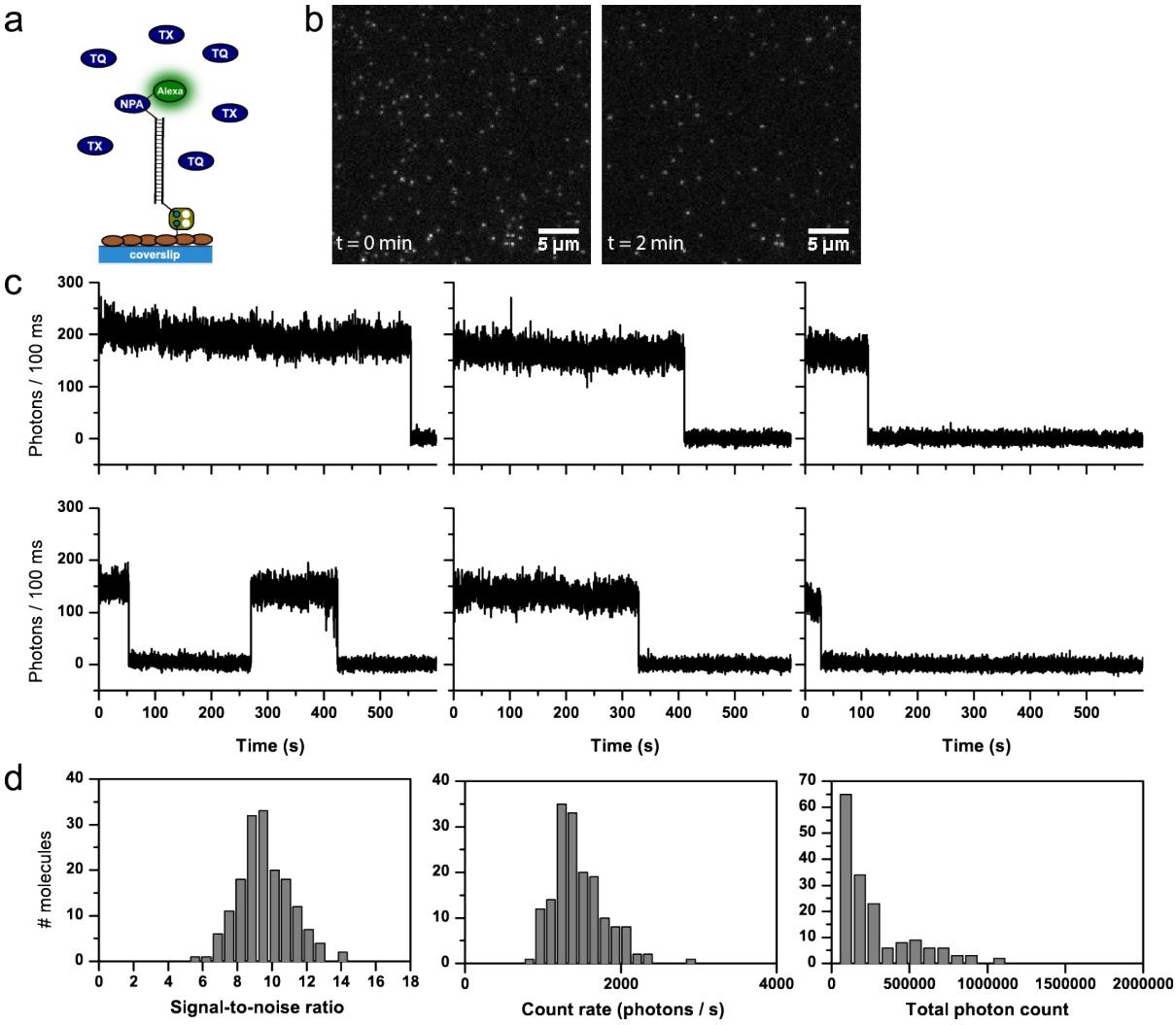

Figure S10: Detailed photophysical characterization of NPA-Alexa555 (buffer with 2 mM TX). a) Schematic representation of photostabilizer-dye conjugates on DNA immobilized on a BSA/BSA-Biotin surface. b) TIRF images at different points in time, brightness and contrast 1888 to 10744 (AD counts). c) Representative time traces. d) Histograms of signal-to-noise ratio, count-rate and total photon count from individual time traces.

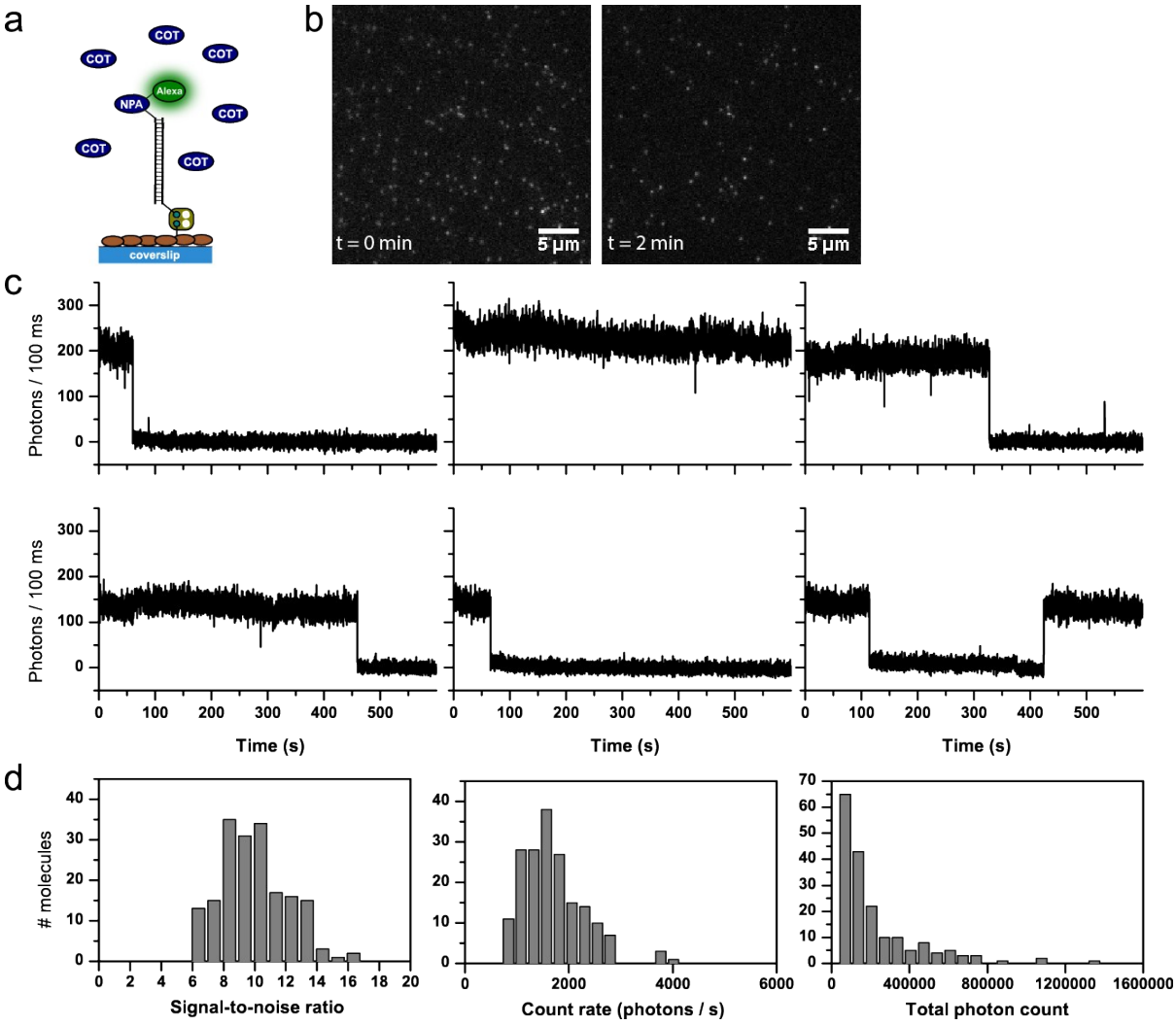

Figure S11: Detailed photophysical characterization of NPA-Alexa555 (buffer with 2 mM COT). a) Schematic representation of photostabilizer-dye conjugates on DNA immobilized on a BSA/BSA-Biotin surface. b) TIRF images at different points in time, brightness and contrast 1939 to 13272 (AD counts). c) Representative time traces. d) Histograms of signal-to-noise ratio, count-rate and total photon count from individual time traces.

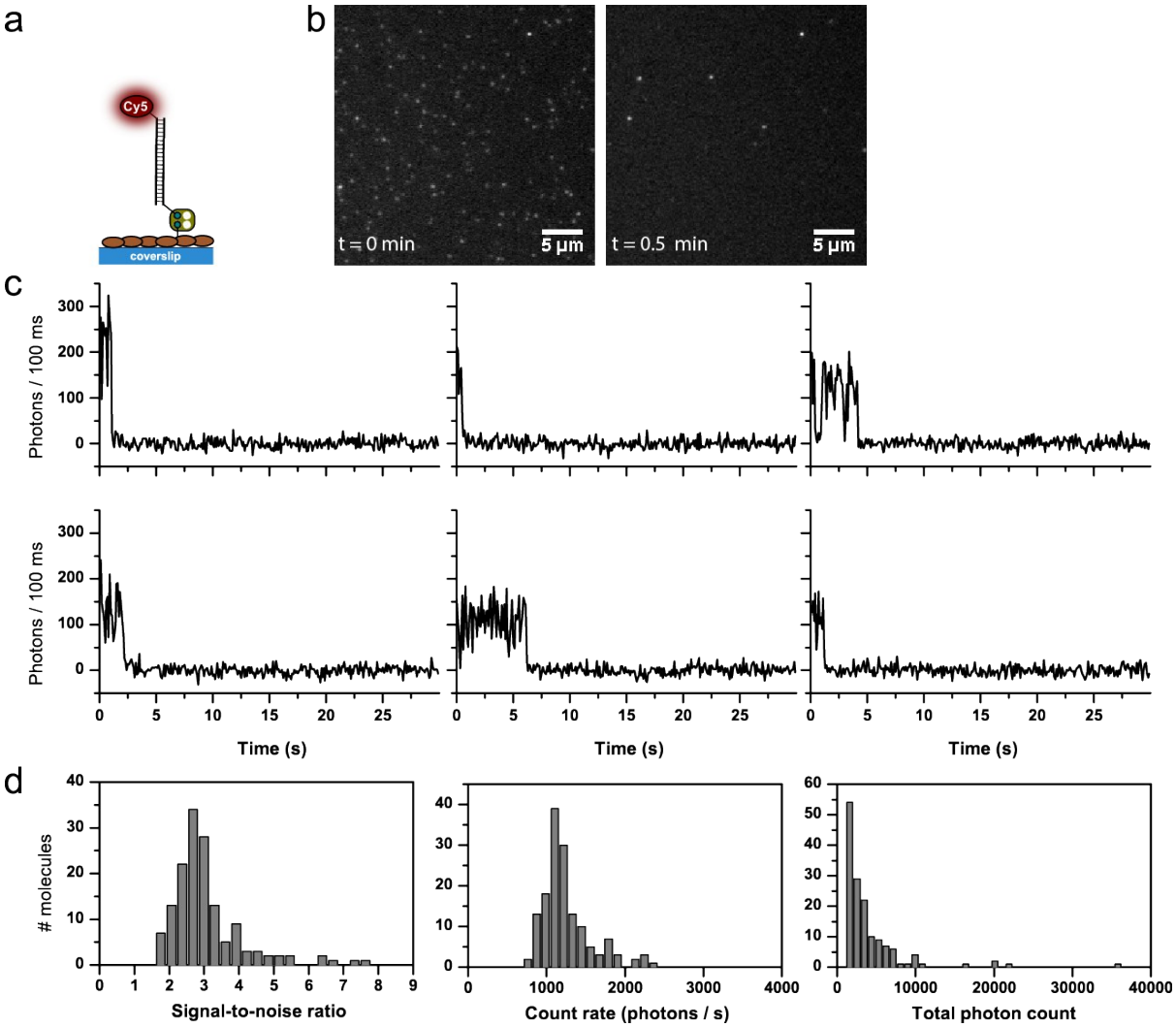

Figure S12: Detailed photophysical characterization of Cy5 (GOX buffer, no photostabilizer in solution**). a)** Schematic representation of dye conjugation on DNA immobilized on a BSA/BSA-Biotin surface. **b) TIRF images at different points in time, brightness and contrast 6766 to 49567 (AD counts). c) Representative time traces. d) Histograms of signal-to-noise ratio, count-rate and total photon count from individual time traces.**

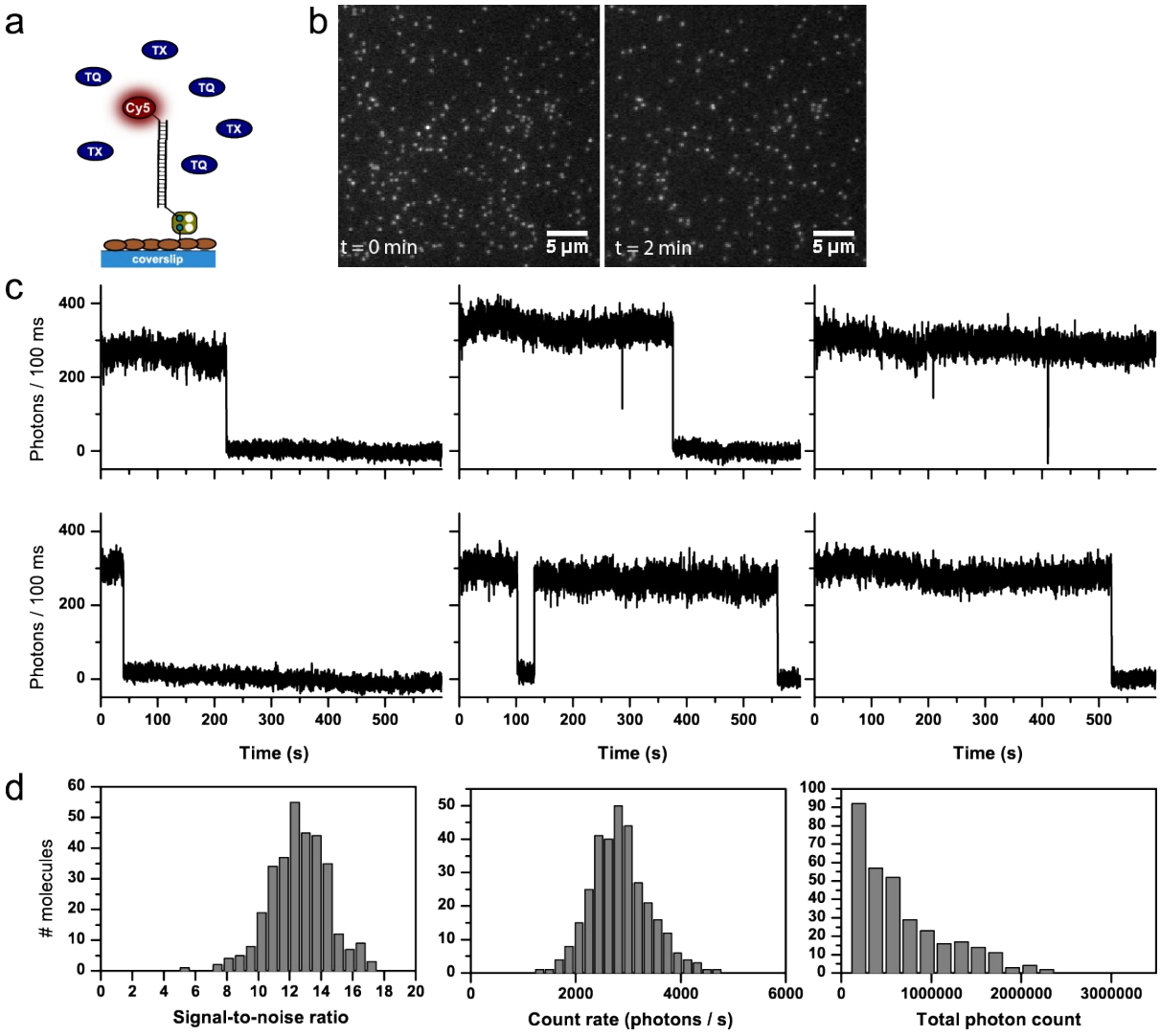

Figure S13: Detailed photophysical characterization of Cy5 (buffer with 2 mM TX). a) Schematic representation of dye conjugation on DNA immobilized on a BSA/BSA-Biotin surface. **b) TIRF images at different points in time, brightness and contrast 6705 to 65535 (AD counts). c) Representative time traces. d) Histograms of signal-to-noise ratio, count-rate and total photon count from individual time traces.**

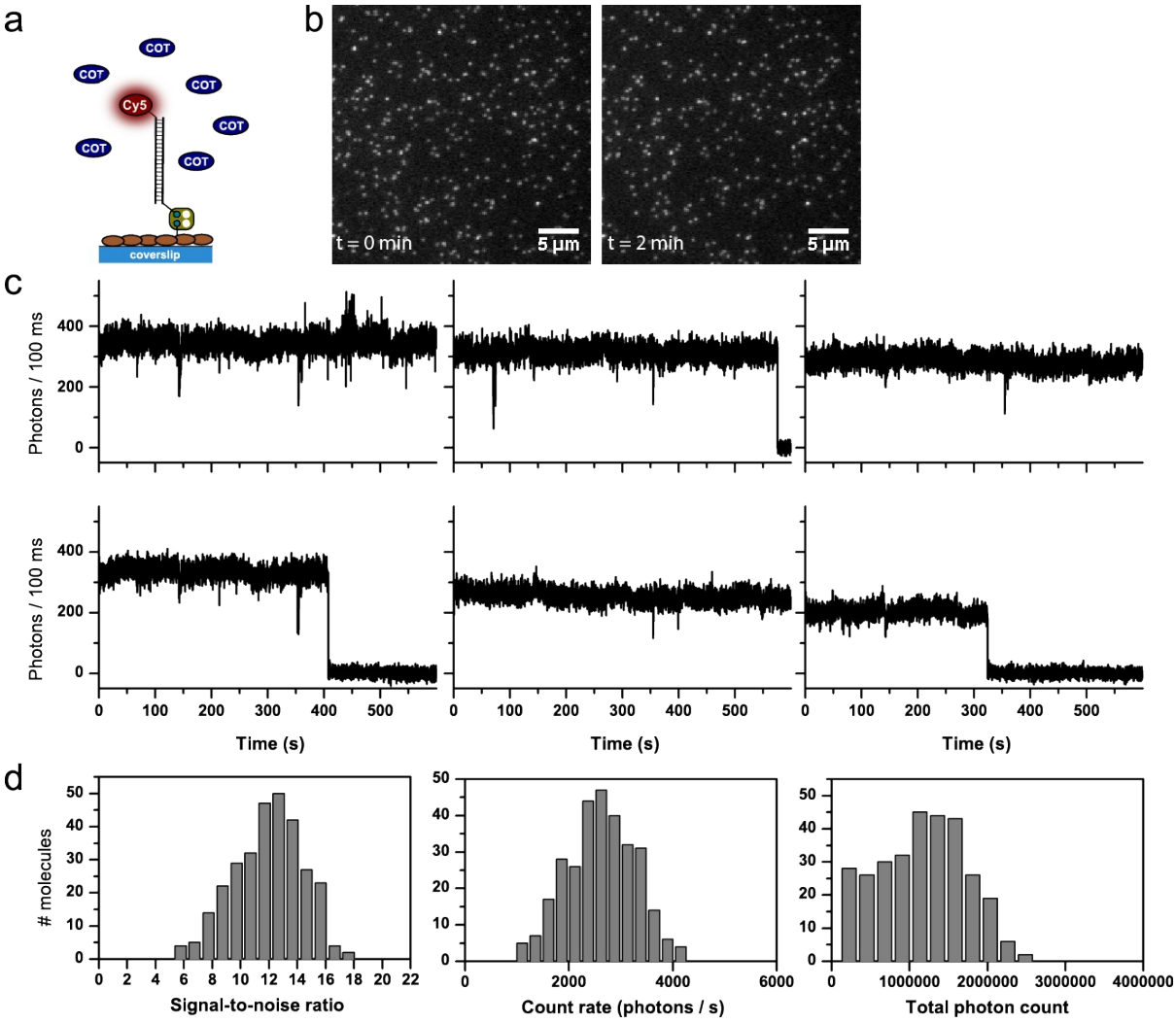

Figure S14: Detailed photophysical characterization of Cy5 (buffer with 2 mM COT). a) Schematic representation of dye conjugation on DNA immobilized on a BSA/BSA-Biotin surface. **b) TIRF images at different points in time, brightness and contrast 8355 to 64081 (AD counts). c) Representative time traces. d) Histograms of signal-to-noise ratio, count-rate and total photon count from individual time traces.**

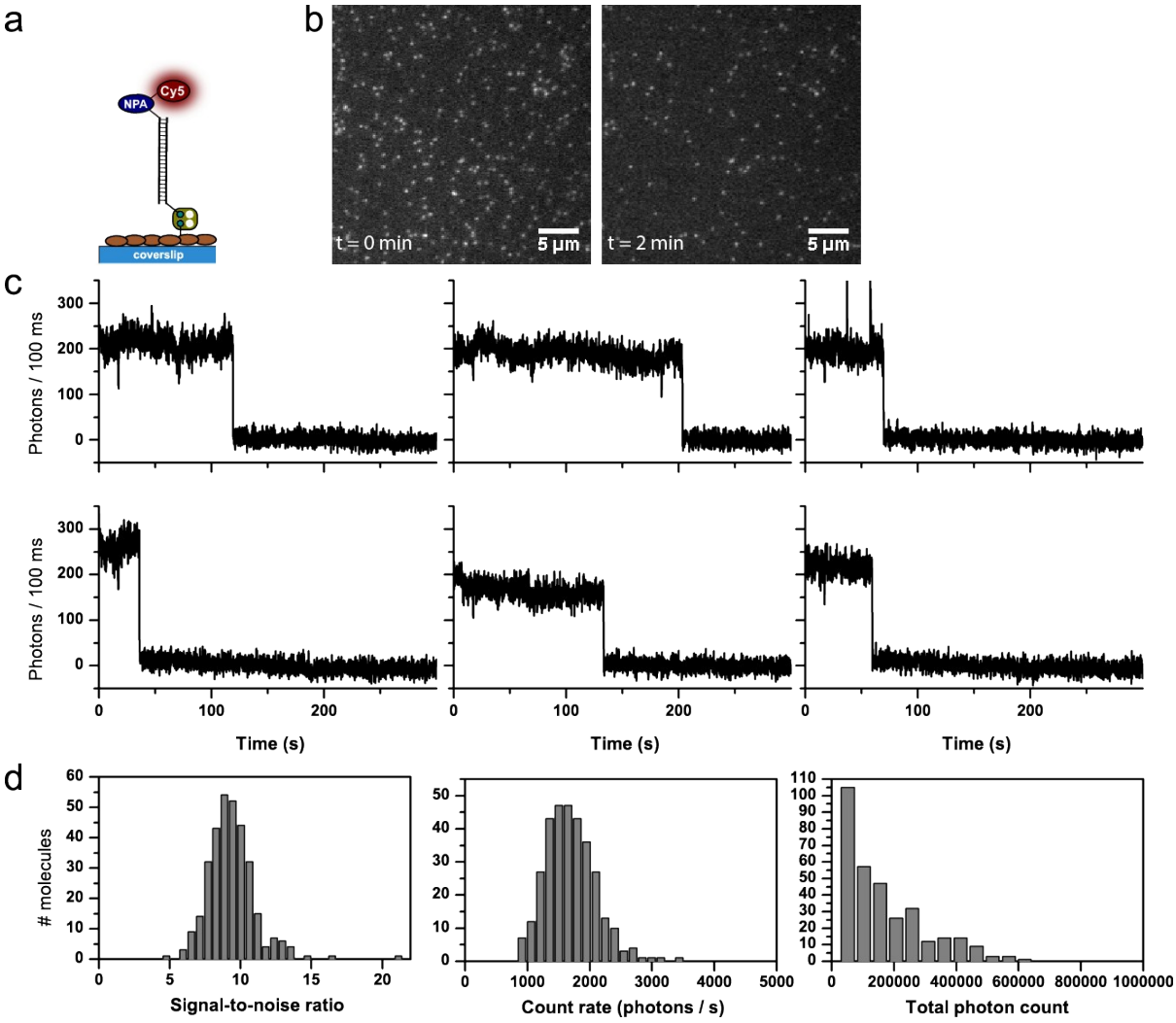

Figure S15: Detailed photophysical characterization of NPA-Cy5 (GOX buffer, no photostabilizer in solution**). a) Schematic representation of photostabilizer-dye conjugates on DNA immobilized on a BSA/BSA-Biotin surface. b) TIRF images at different points in time, brightness and contrast 5820 to 43075 (AD counts). c) Representative time traces. d) Histograms of signal-to-noise ratio, count-rate and total photon count from individual time traces.**

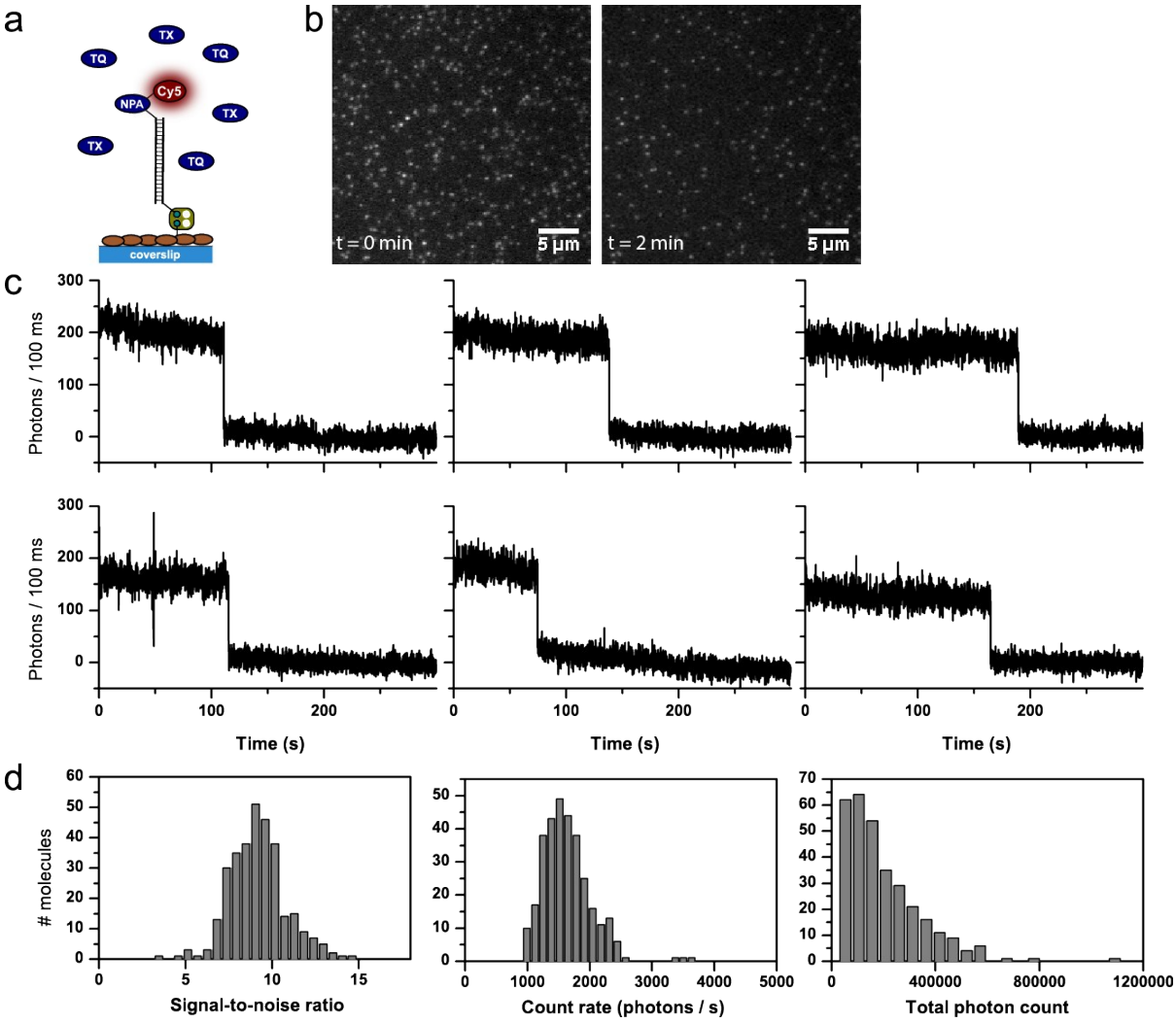

Figure S16: Detailed photophysical characterization of NPA-Cy5 (buffer with 2 mM TX). a) Schematic representation of photostabilizer-dye conjugates on DNA immobilized on a BSA/BSA-Biotin surface. b) TIRF images at different points in time, brightness and contrast 7408 to 52325 (AD counts). c) Representative time traces. d) Histograms of signal-to-noise ratio, count-rate and total photon count from individual time traces.

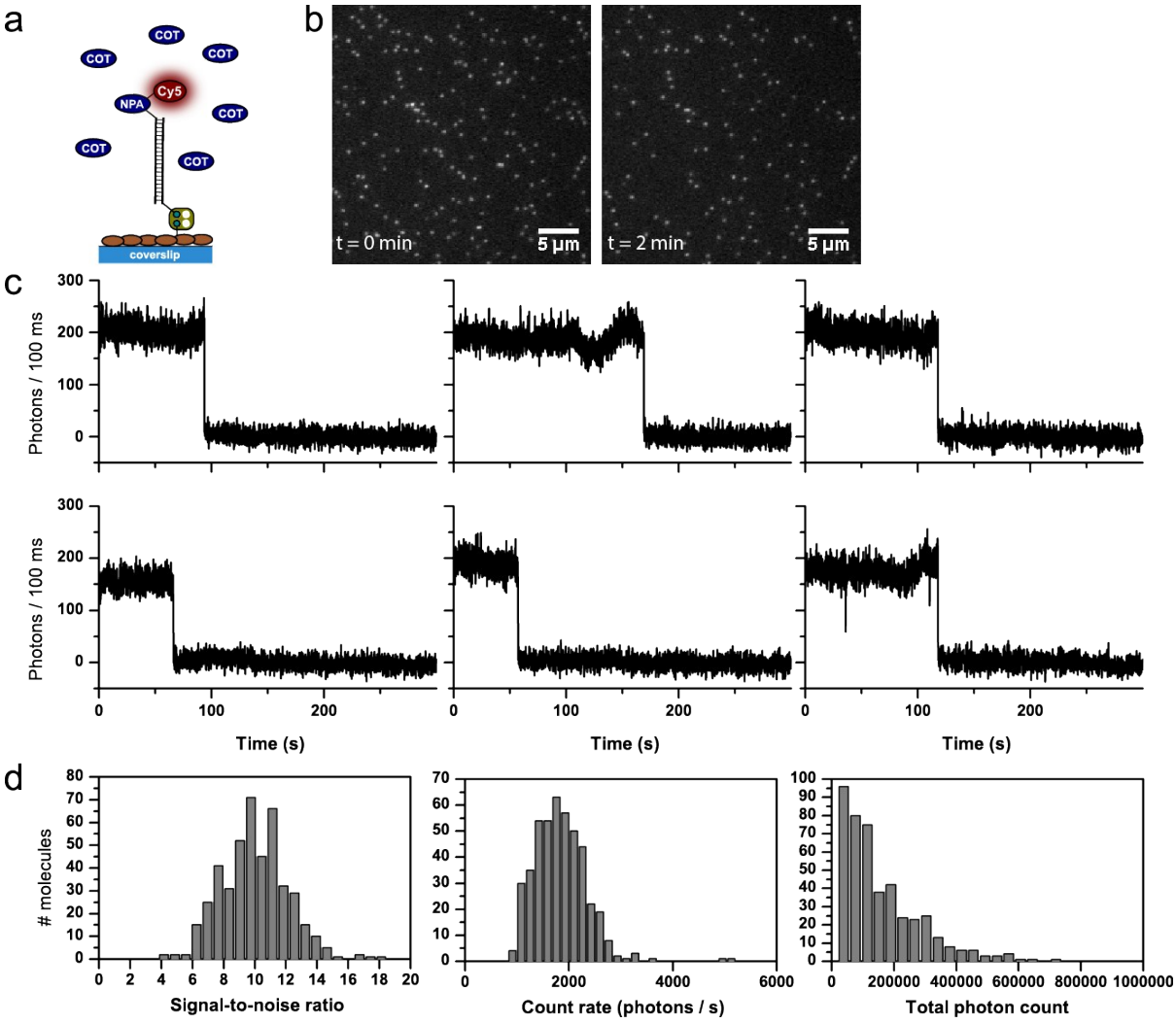

Figure S17: Detailed photophysical characterization of NPA-Cy5 (buffer with 2 mM COT). a) Schematic representation of photostabilizer-dye conjugates on DNA immobilized on a BSA/BSA-Biotin surface. b) TIRF images at different points in time, brightness and contrast 8342 to 54037 (AD counts). c) Representative time traces. d) Histograms of signal-to-noise ratio, count-rate and total photon count from individual time traces.

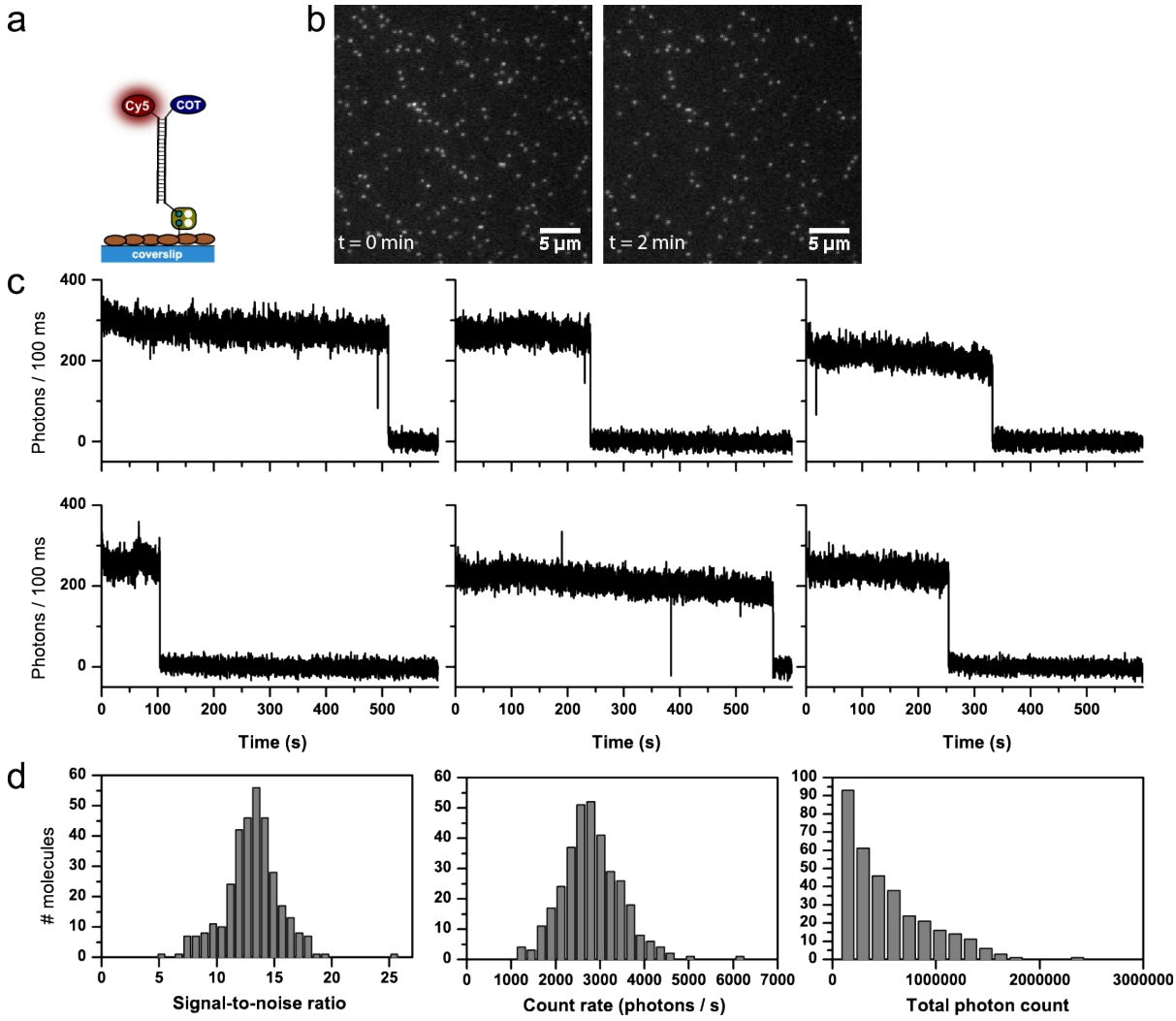

Figure S18: Detailed photophysical characterization of Cy5-COT (GOX buffer, no photostabilizer in solution**). a) Schematic representation of photostabilizer-dye conjugates on DNA immobilized on a BSA/BSA-Biotin surface. b) TIRF images at different points in time, brightness and contrast 6413 to 60344 (AD counts). c) Representative time traces. d) Histograms of signal-to-noise ratio, count-rate and total photon count from individual time traces.**

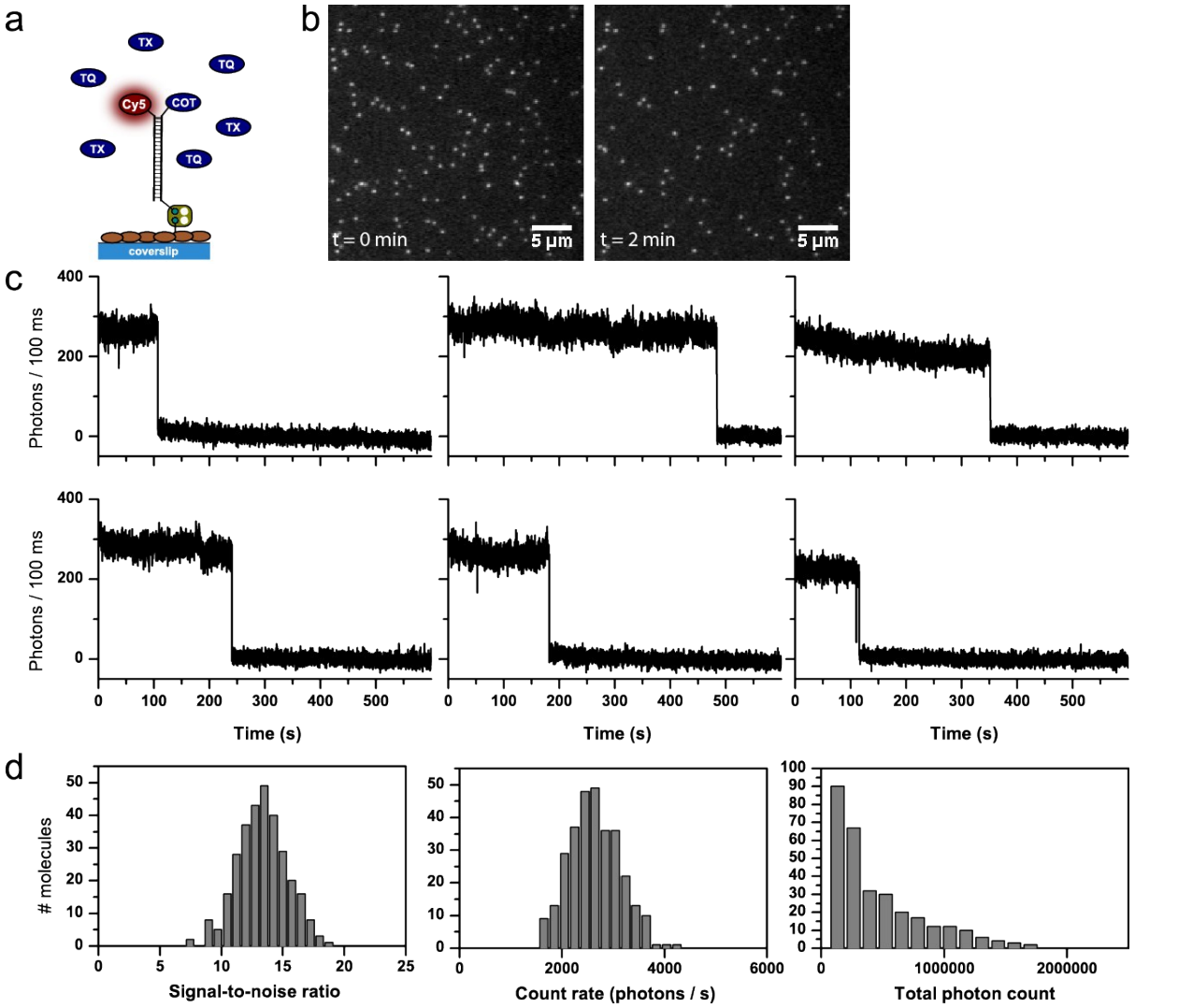

Figure S19: Detailed photophysical characterization of Cy5-COT (buffer with 2 mM TX). a) Schematic representation of photostabilizer-dye conjugates on DNA immobilized on a BSA/BSA-Biotin surface. b) TIRF images at different points in time, brightness and contrast 8143 to 62500 (AD counts). c) Representative time traces. d) Histograms of signal-to-noise ratio, count-rate and total photon count from individual time traces.

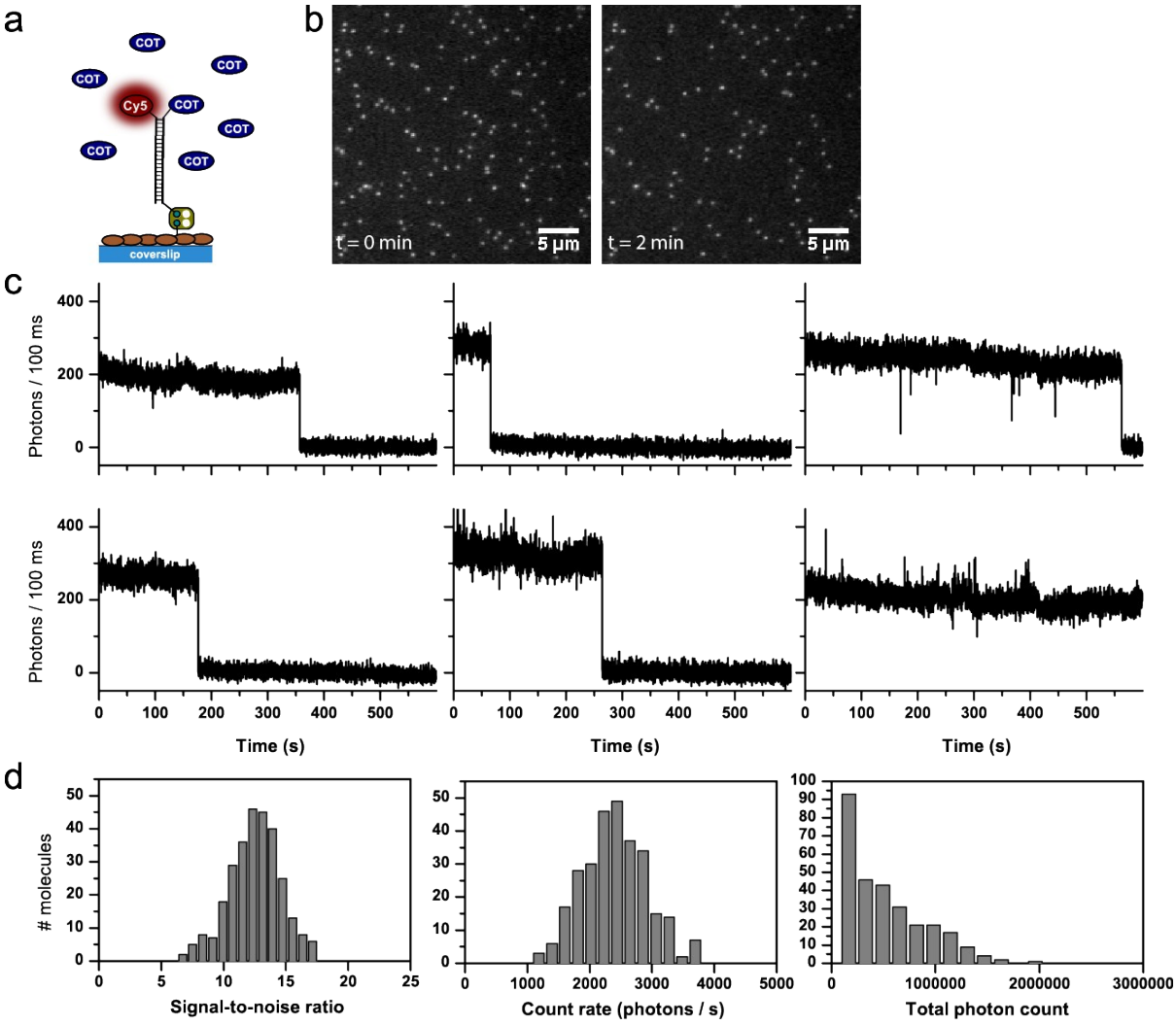

Figure S20: Detailed photophysical characterization of Cy5-COT (buffer with 2 mM TX). a) Schematic representation of photostabilizer-dye conjugates on DNA immobilized on a BSA/BSA-Biotin surface. b) TIRF images at different points in time, brightness and contrast 7804 to 44206 (AD counts). c) Representative time traces. d) Histograms of signal-to-noise ratio, count-rate and total photon count from individual time traces.

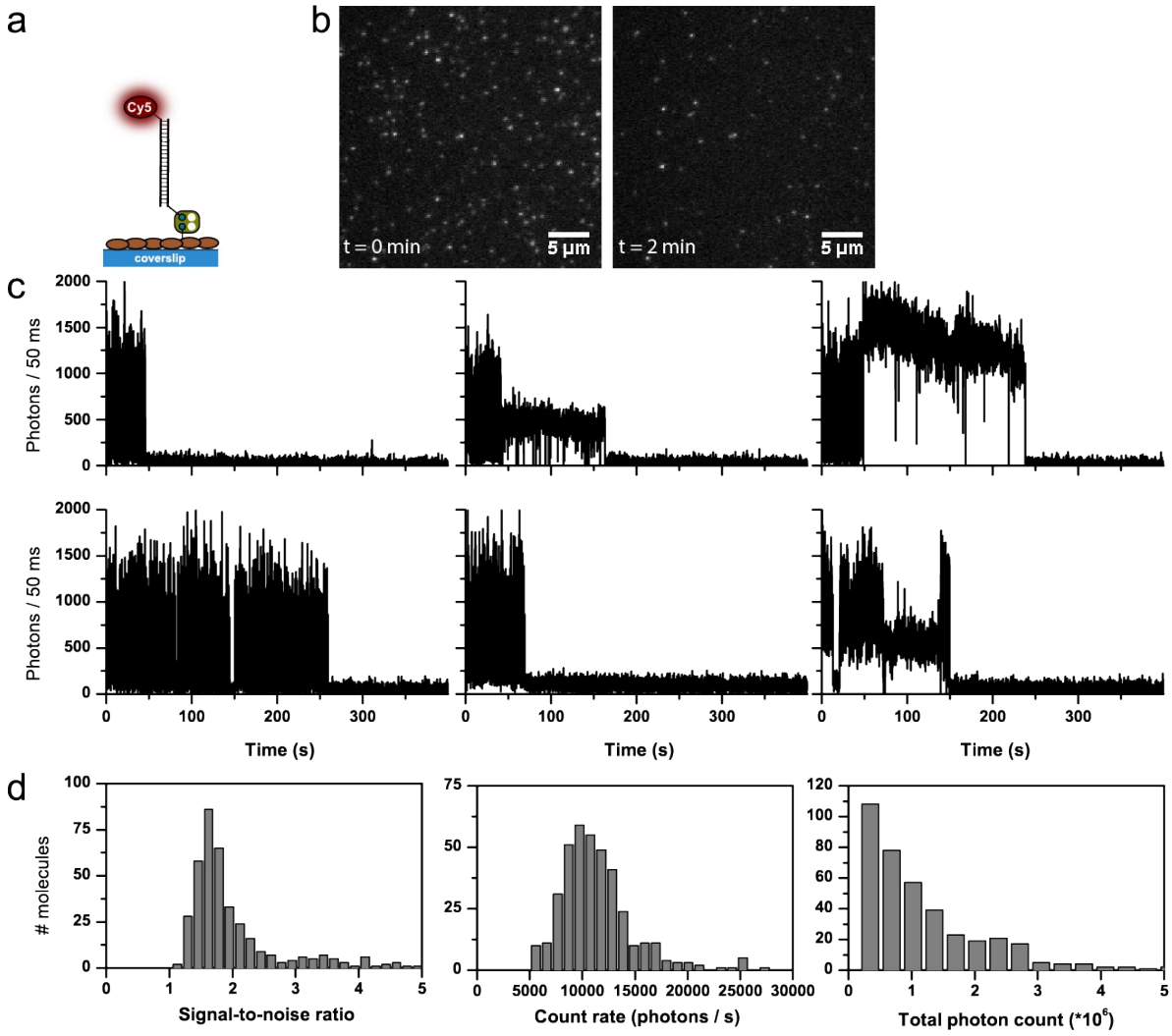

Figure S21: Detailed photophysical characterization of Cy5 (GOX buffer, no photostabilizer in solution**) as a control experiment for Figures S23-S24. a)** Schematic representation of dye conjugation on DNA immobilized on a BSA/BSA-Biotin surface. **b) TIRF images at different points in time, brightness and contrast 3396 to 50600 (AD counts). c) Representative time traces. d) Histograms of signal-to-noise ratio, count-rate and total photon count from individual time traces.**

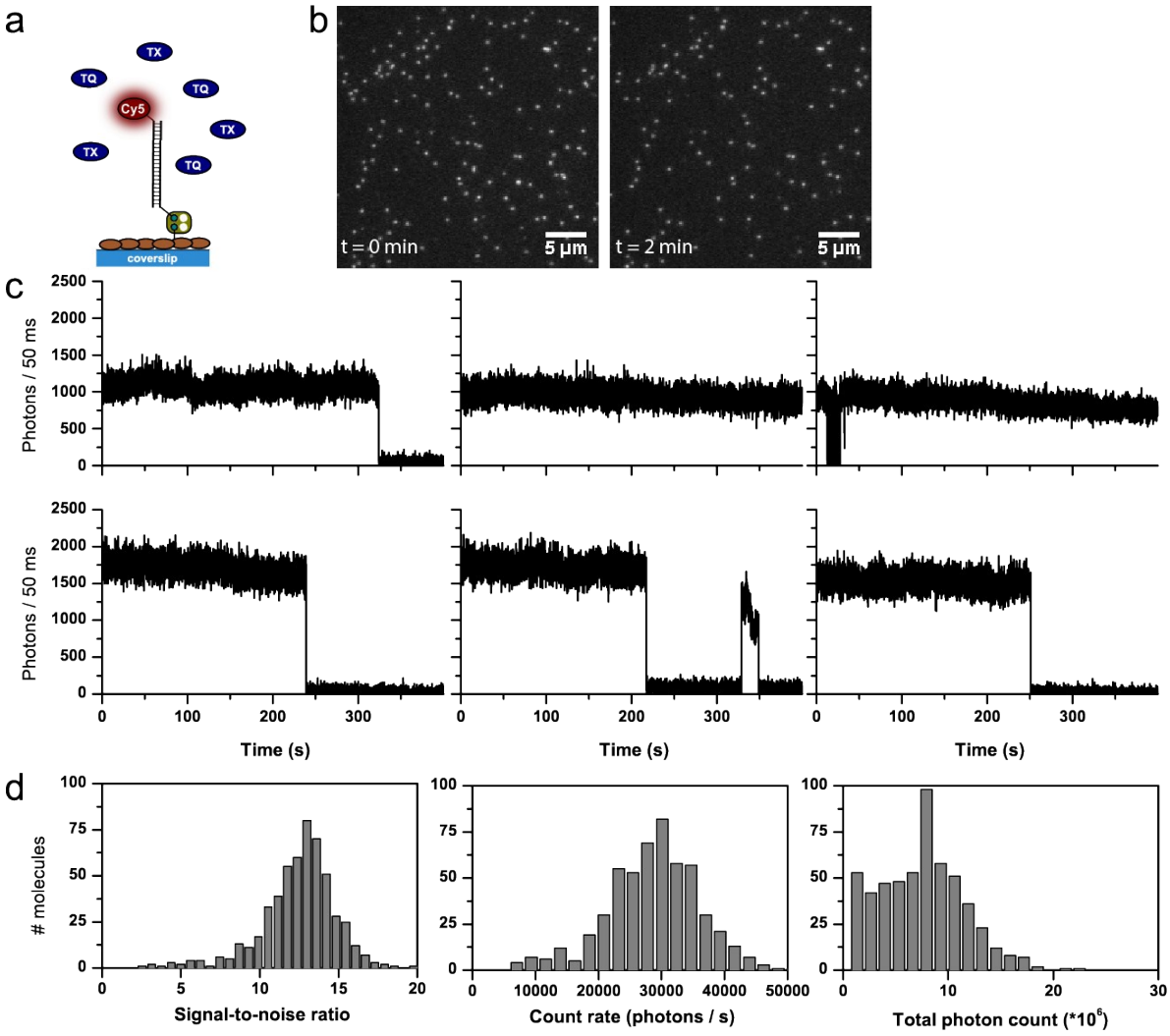

Figure S22: Detailed photophysical characterization of Cy5 (buffer with 2 mM TX) as a control experiment for Figures S23-S24. a) Schematic representation of dye conjugation on DNA immobilized on a BSA/BSA-Biotin surface. b) TIRF images at different points in time, brightness and contrast 3147 to 65535 (AD counts). c) Representative time traces. d) Histograms of signal-to-noise ratio, count-rate and total photon count from individual time traces.

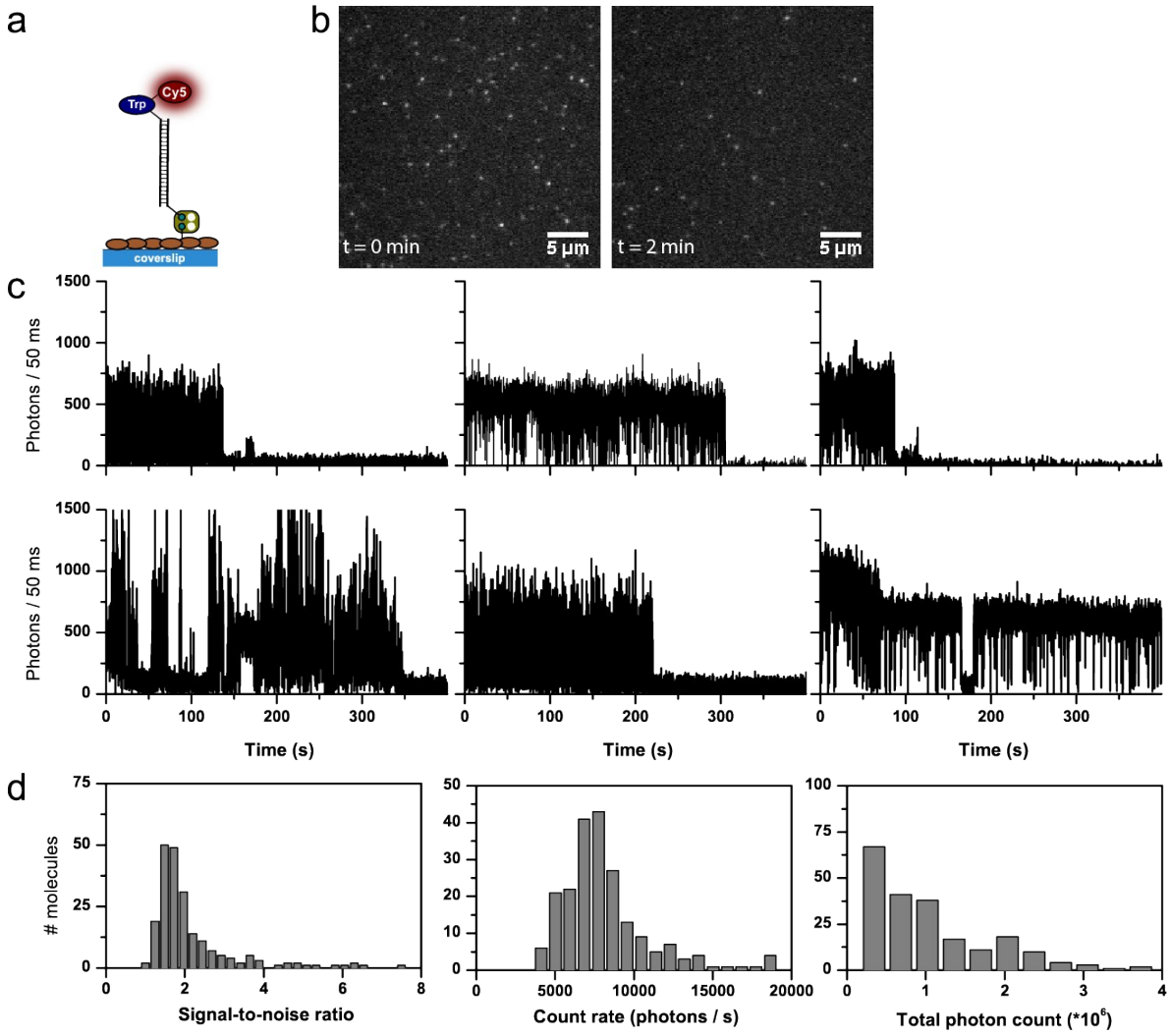

Figure S23: Detailed photophysical characterization of Trp-Cy5 (GOX buffer, no photostabilizer in solution**). a) Schematic representation of Trp-dye conjugate on DNA immobilized on a BSA/BSA-Biotin surface. b) TIRF images at different points in time, brightness and contrast 2990 to 29808 (AD counts). c) Representative time traces. d) Histograms of signal-to-noise ratio, count-rate and total photon count from individual time traces.**

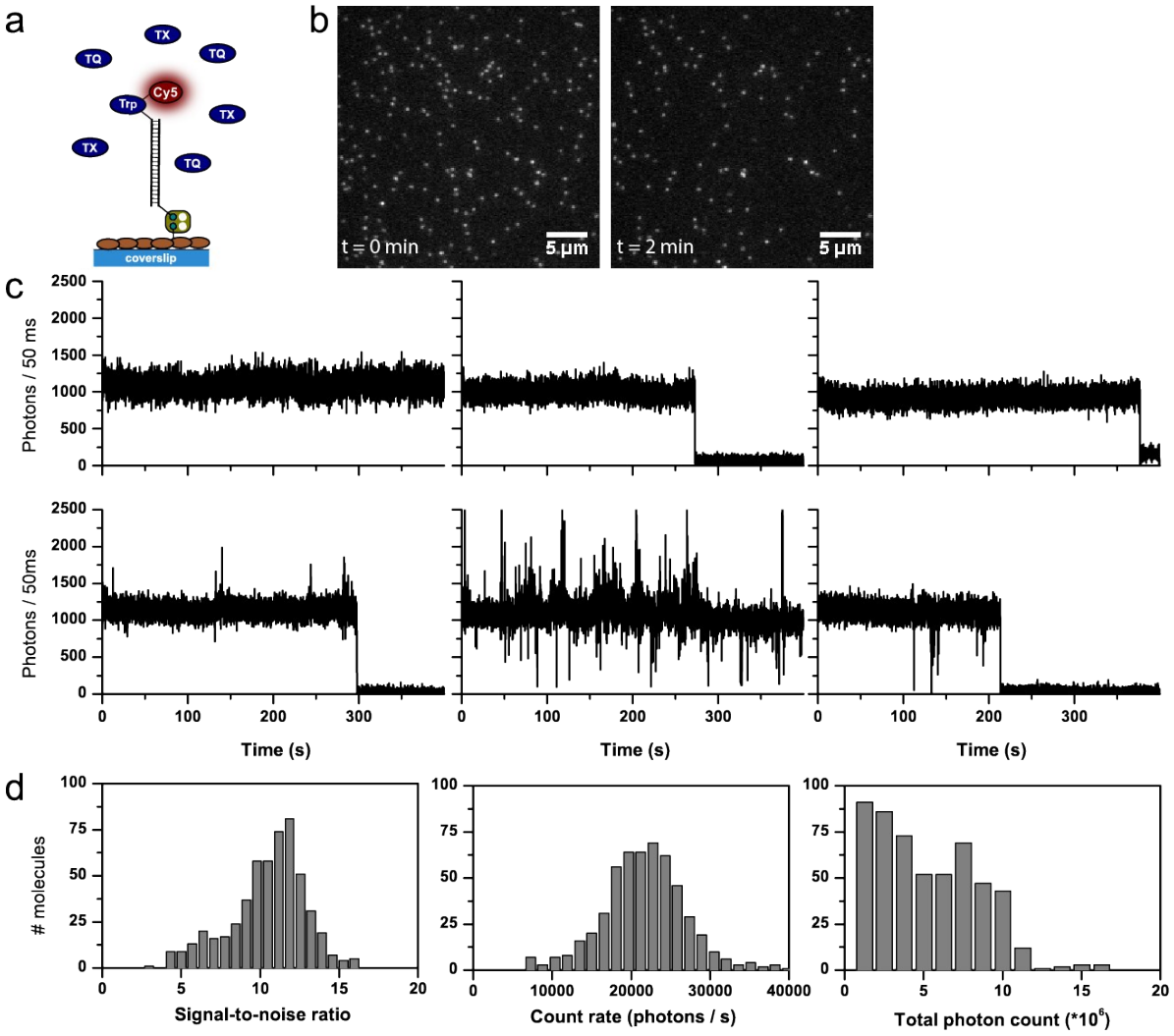

Figure S24: Detailed photophysical characterization of Trp-Cy5 (buffer with 2 mM TX). a) Schematic representation of Trp-dye conjugate on DNA immobilized on a BSA/BSA-Biotin surface. b) TIRF images at different points in time, brightness and contrast 3627 to 50895 (AD counts). c) Representative time traces. d) Histograms of signal-to-noise ratio, count-rate and total photon count from individual time traces.

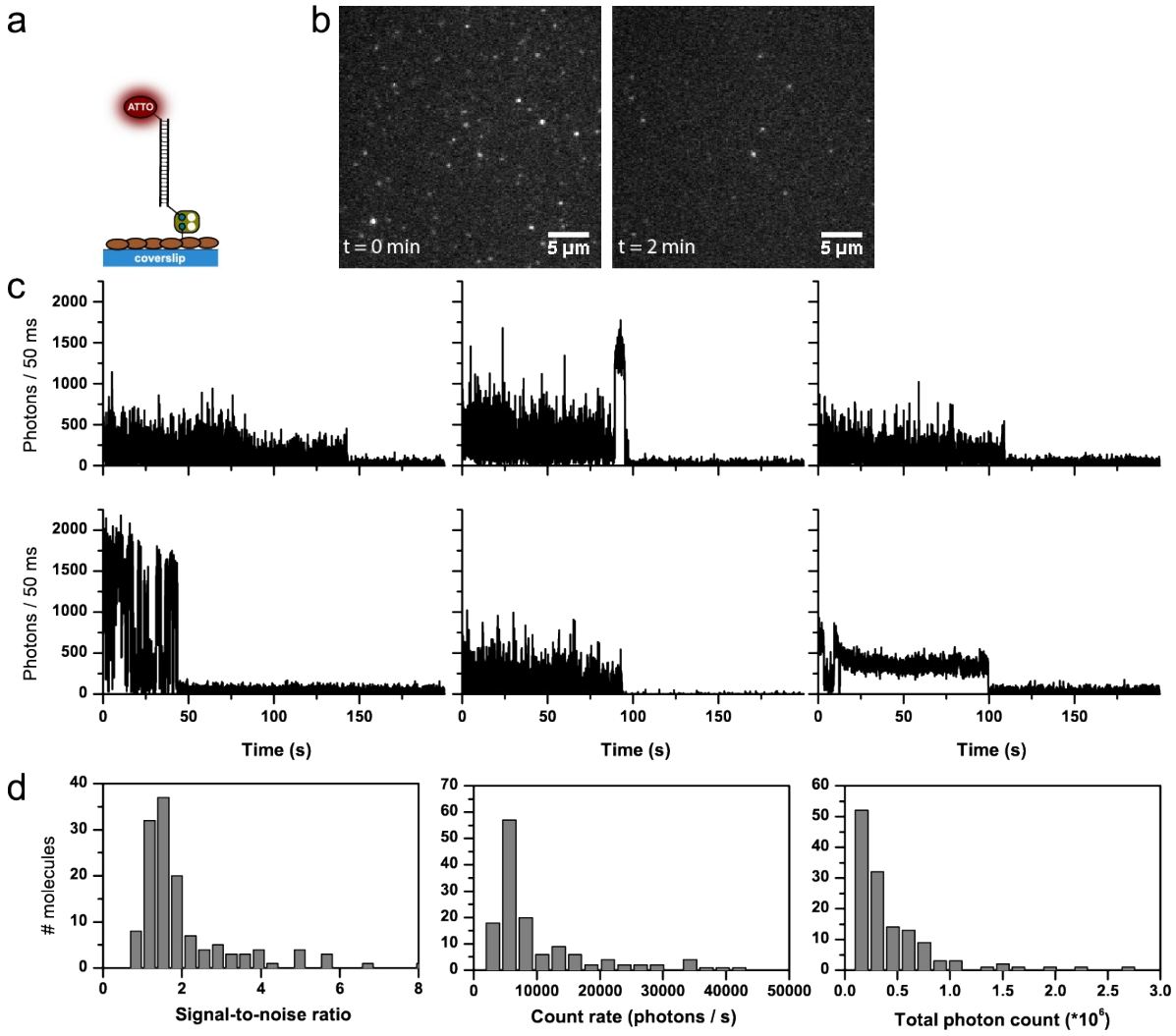

Figure S25: Detailed photophysical characterization of ATTO647N (GOX buffer, no photostabilizer in solution**) as a control experiment for Figures S27-S28. a) Schematic representation of dye conjugation on DNA immobilized on a BSA/BSA-Biotin surface. b) TIRF images at different points in time, brightness and contrast 3031 to 26808 (AD counts). c) Representative time traces. d) Histograms of signal-to-noise ratio, count-rate and total photon count from individual time traces.**

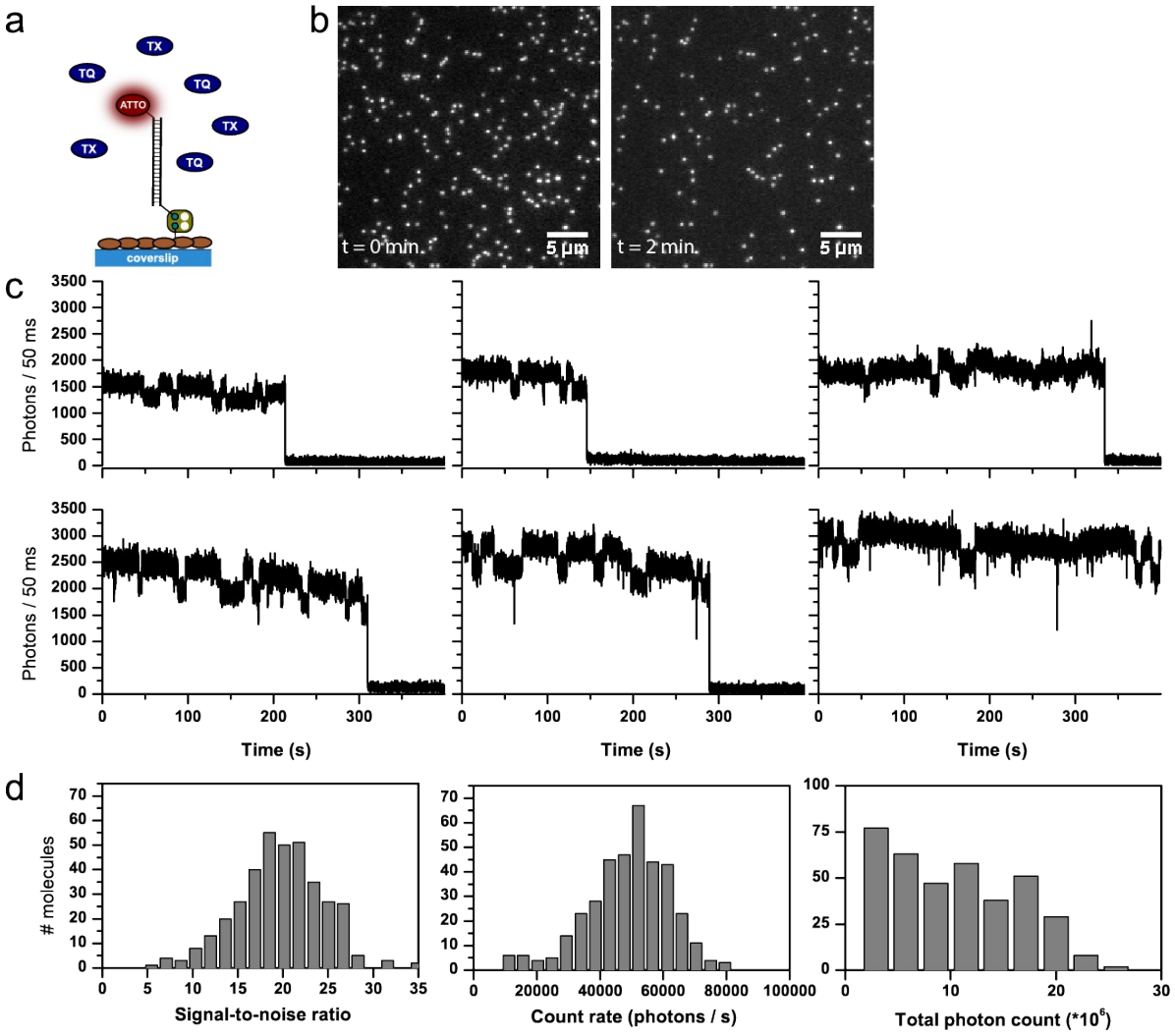

Figure S26: Detailed photophysical characterization of ATTO647N (buffer with 2 mM TX) as a control experiment for Figures S27-S28. a) Schematic representation of dye conjugation on DNA immobilized on a BSA/BSA-Biotin surface. b) TIRF images at different points in time, brightness and contrast 4400 to 65535 (AD counts). c) Representative time traces. d) Histograms of signal-to-noise ratio, count-rate and total photon count from individual time traces.

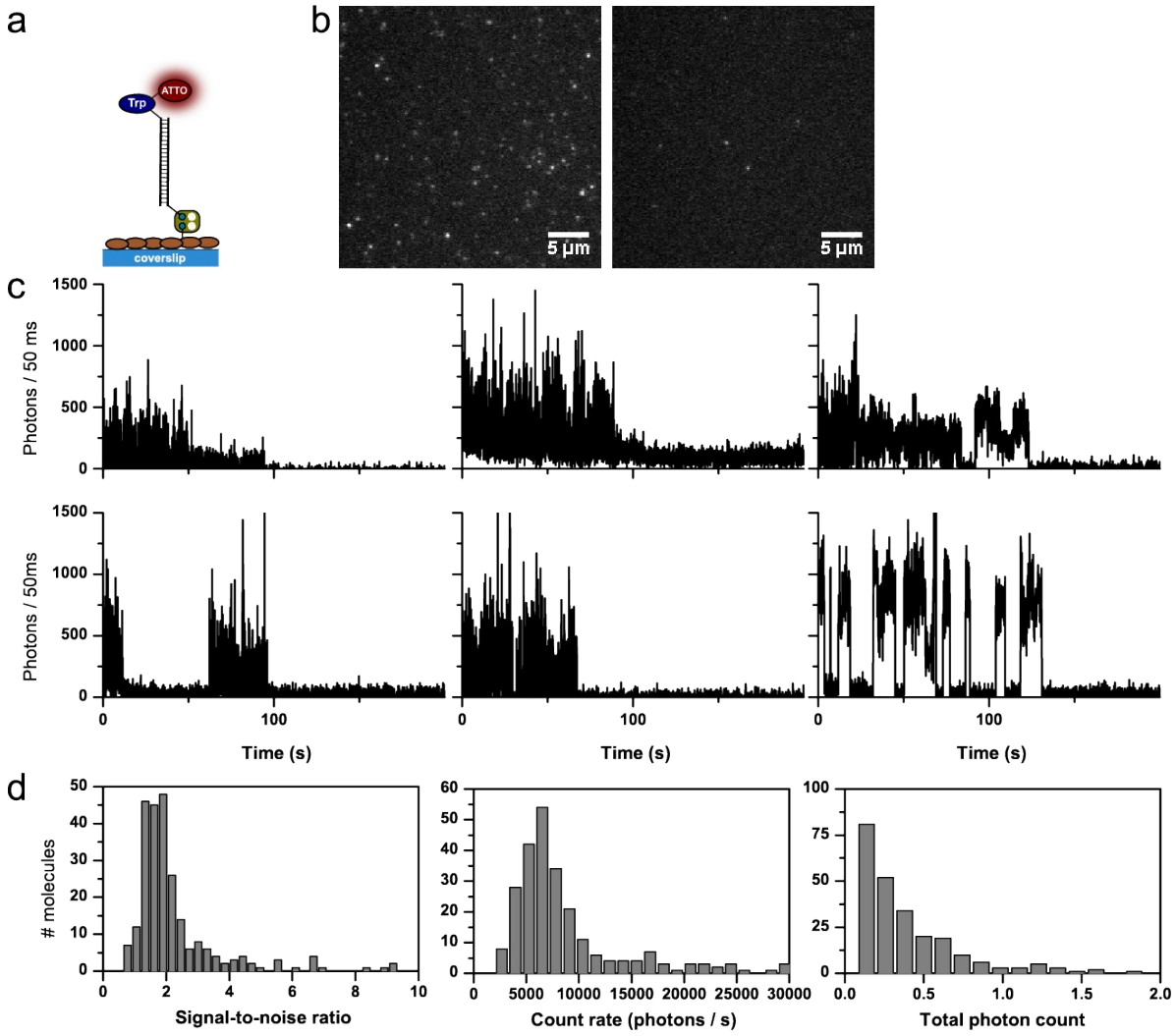

Figure S27: Detailed photophysical characterization of Trp-ATTO647N (GOX buffer, no photostabilizer in solution**). a) Schematic representation of Trp-dye conjugates on DNA immobilized on a BSA/BSA-Biotin surface. b) TIRF images at different points in time, brightness and contrast 3780 to 35441 (AD counts). c) Representative time traces. d) Histograms of signal-to-noise ratio, count-rate and total photon count from individual time traces.**

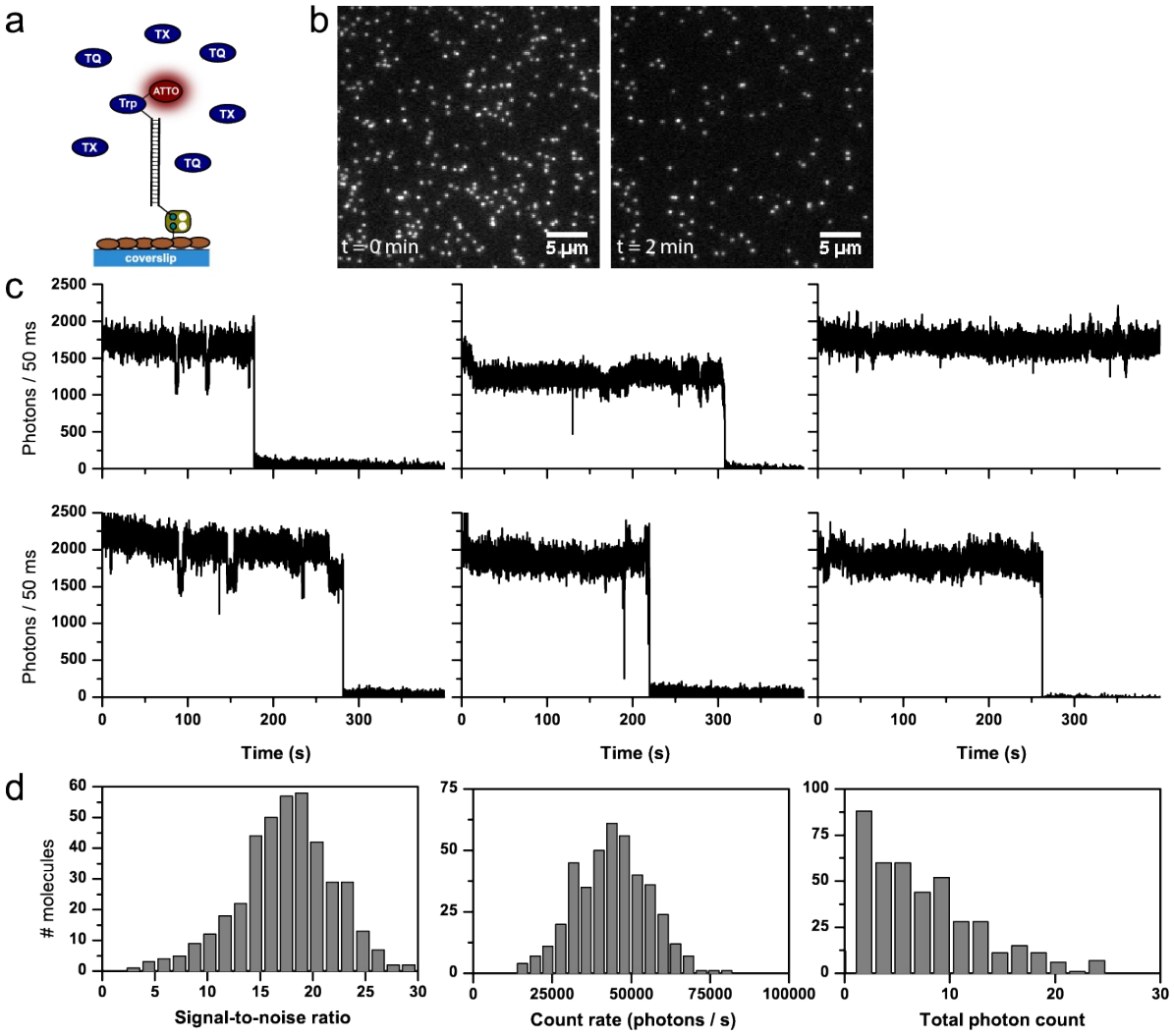

Figure S28: Detailed photophysical characterization of Trp-ATTO647N (buffer with 2 mM TX). a) Schematic representation of Trp-dye conjugate on DNA immobilized on a BSA/BSA-Biotin surface. b) TIRF images at different points in time, brightness and contrast 4686 to 65535 (AD counts). c) Representative time traces. d) Histograms of signal-to-noise ratio, count-rate and total photon count from individual time traces.

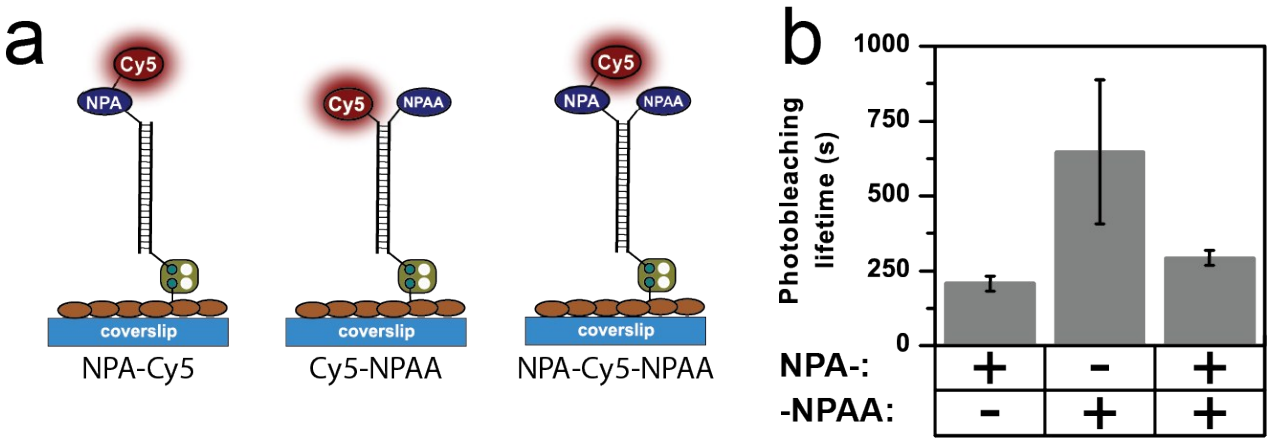

Figure S29: Comparison of Cy5 photostability with different geometries of intramolecular photostabilization by NPA and a combination of both. Error bar show standard deviation of repeats on 3 different days.

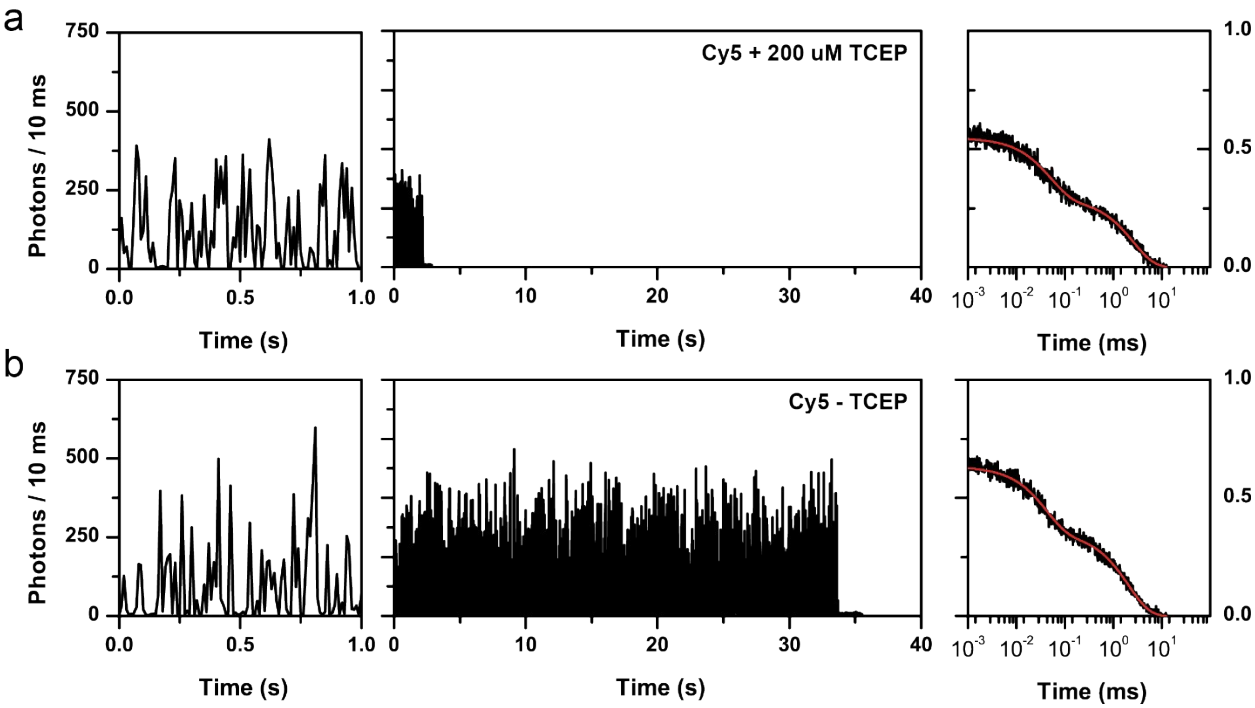

Figure S30: Confocal microscopy transients of Cy5 and autocorrelation a) in the presence of 200 uM TCEP and b) absence of TCEP. The autocorrelation function (ACF) of a) was obtained by summation of 88 individual ACFs while in panel b the fluorescent transient shown was used to calculate the ACF. The fit is shown in red from which revealed off-times of a) 8.7 ± 2.8 ms 75 ± 15 µs, b) 9.5 ± 0.7 ms and 73 ± 18 µs.

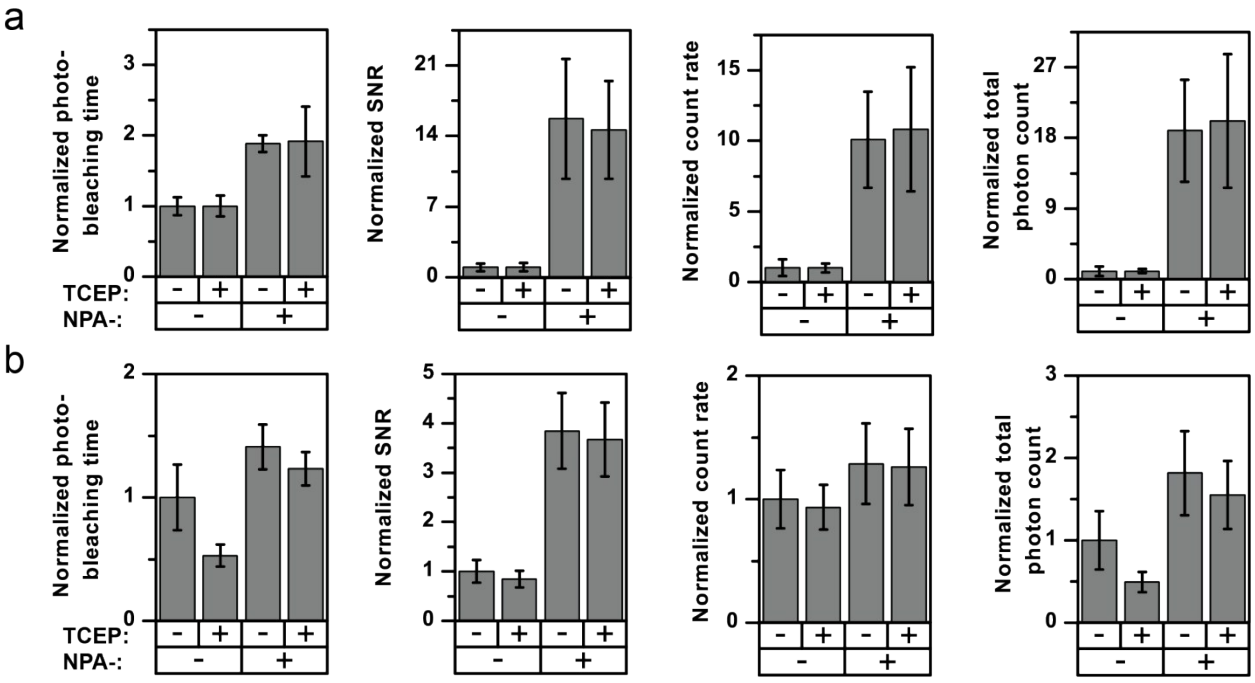

Figure S31: Photophysical characterization of a) ATTO647N and NPA-ATTO647 b) Alexa555 and NPA-Alexa555 in the absence or presence of 200 µM TCEP. All imaging was done under deoxygenated conditions with 400 W cm^{-2} excitation at a) 637 nm or b) 523 nm. Error bars show standard deviation of repeats on 3 different days.

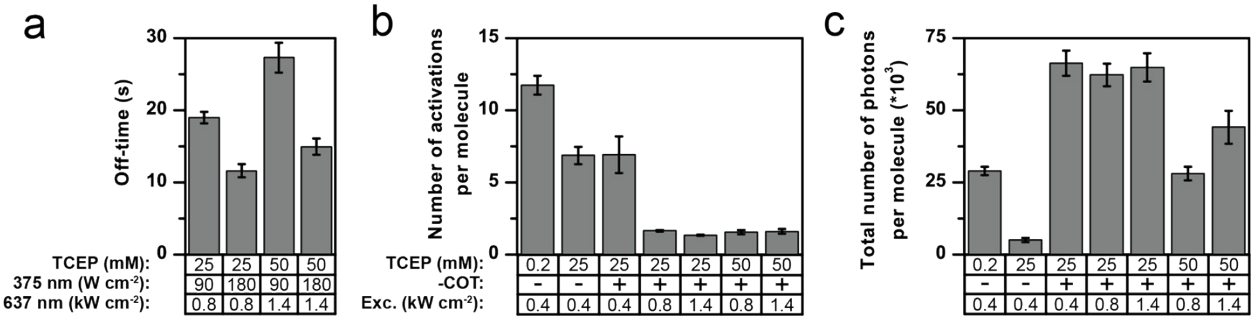

Figure S32: Additional parameters for COT-Cy5 photoactivation using TCEP as photoswitching agent. a) Mean off times between successive activations as a function of 375 nm activation laser power. b) Mean number of activation events per molecule c) Total number of photons detected per activated molecule.

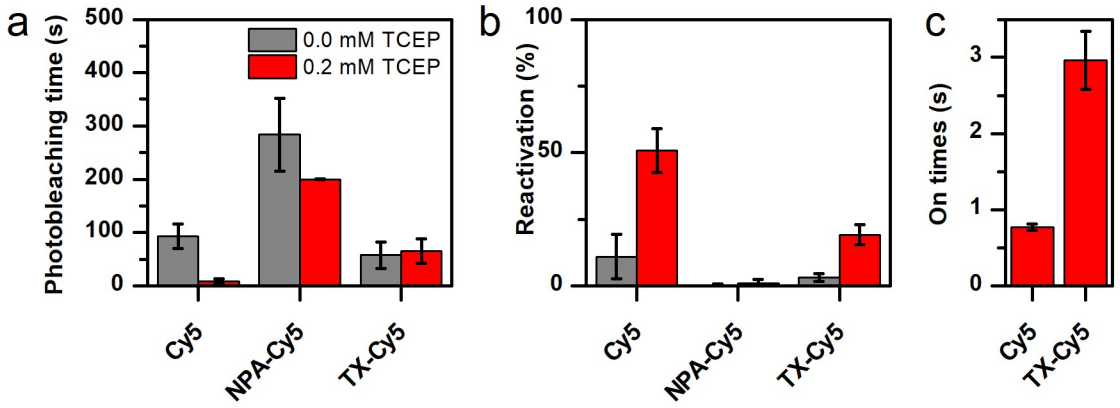

Figure S33: Photoactivation parameters of NPA-Cy5 and TX-Cy5 compared to parent fluorophore Cy5 in the presence and absence of 0.2 mM TCEP, showing (a) Apparent photobleaching time, (b) percentage of fluorophores activated, and (c) on-times of conditions with significant activation. Error bars are standard deviation of repeats (a, b) or SEM (c).

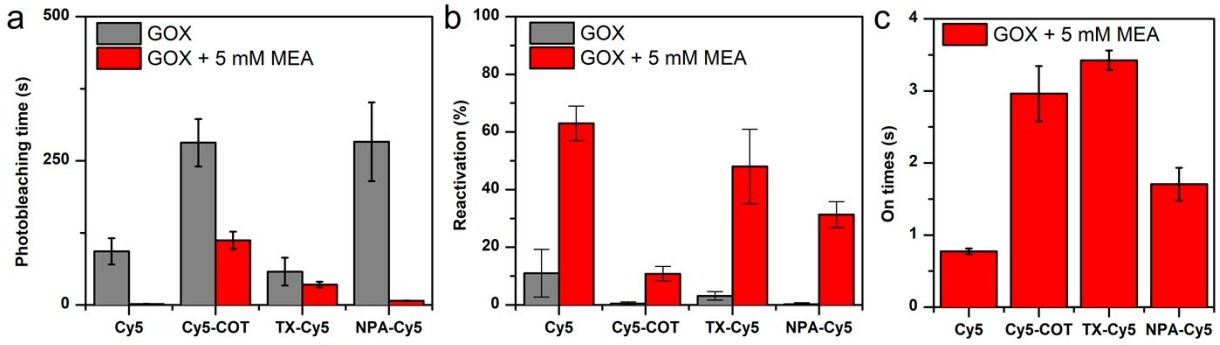

Figure S34: Photoactivation parameters of Cy5-COT, NPA-Cy5 and TX-Cy5 compared to parent fluorophore Cy5 in the presence and absence of 5 mM MEA (cysteamine), showing (a) Apparent photobleaching time, (b) percentage of fluorophores activated, and (c) on-times of conditions with significant activation. Error bars are standard deviation of repeats (a, b) or SEM (c).

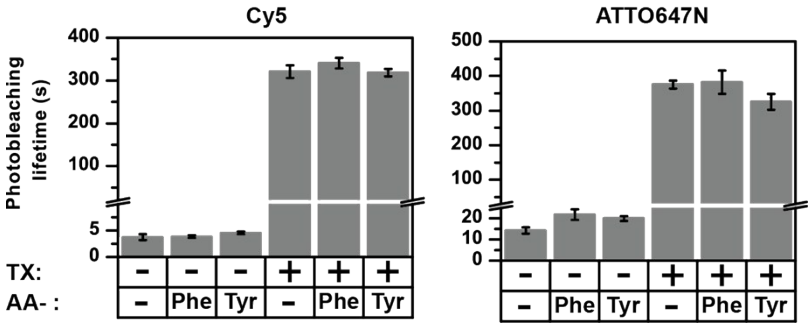

Figure S35: Photobleaching lifetimes of (a) Cy5 and (b) ATTO647N, showing the influence of covalently coupled phenylalanine and tyrosine in the absence and presence of 2 mM TX. All measurements were done in the absence of oxygen with 637 nm excitation (800 W cm^{-2}). Error bars show standard deviation of repeats on 2 different days. Labelled ssDNA samples were prepared as described previously using amino-acid scaffolding.[2]

1. Details of chemical synthesis

Synthesis of the brominated cyclooctatetraene via a modified literature procedure.[1]

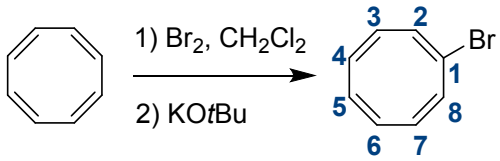

1-Bromocyclooctratetraene (1): A solution of cyclooctatetraene (1.0 mL, 8.68 mmol) in DCM (10 mL) was cooled to -70 °C under argon atmosphere. At this point, bromine (0.46 mL, 8.95 mmol) in 6 mL DCM was added dropwise to the reaction mixture and stirred for 1.5 h. Then, a solution of KO*t*Bu (2.37 g, 12.2 mmol) in 6 mL THF was slowly added drop by drop to the solution, warmed to -60 °C and stirred for additionally 4 h. The reaction mixture was warmed to -10 °C, poured into ice water and the aqueous layer was extracted with cooled diethyl ether (3 x 5 mL). The combined organic phases were dried over $MgSO_4$, filtered and concentrated to obtain a brownish oil without purification. Yield 1.24 g, (6.77 mmol, 78%)

TLC: DCM/MeOH 95:5, R_f **(1)** = 0.98.

^{1}H NMR (400 MHz, $CDCl_3$) δ = 6.22 (s, 1H, H-8), 5.98 – 5.74 (m, 5H, H-3, H-4, H-5, H-6, H-7), 5.67-5.60 (m, 1H, H-2) ppm.

^{13}C-NMR (400 MHz, CDCl3): δ 133.4 1(C), 133.3 (1C), 133.0 (1C), 132.6 (1C), 132.3 (1C), 131.1 (2C), 121.6 (1C) ppm.

HRMS (M+H+) calculated for C_8H_7Br 182.9804 g mol^{-1}, found 182.9803 g mol^{-1}.

Synthesis of the alcohol derivative of cyclooctatetraene

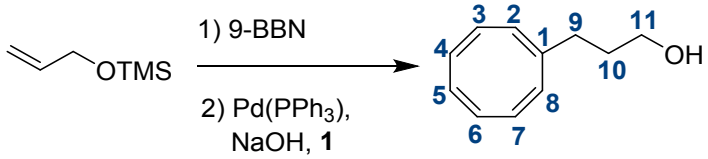

Cyclooctatetraenyl-propanol (2) Allyloxytrimethylsilane (1.0 mL, 5.93 mmol) in 5 mL dry THF and 9-BBN (13 mL, ~ 6.5 mmol) were stirred at 0° C under argon for 2.5 h. Then, $Pd(PPh_3)_4$ (100.3 mg, 0.09 mmol), 5 mL 3 M NaOH and **1** (1.3 g, 7.10 mmol) were added and the reaction mixture was refluxed for 15 h. Afterwards, the mixture was cooled and diluted with hex/EtOAc (1:1), washed with brine and water, dried over $MgSO_4$ and concentrated. The crude product was purified by column chromatography (SiO_2, DCM/MeOH 97:3) to yield a yellowish oil. Yield: 0.639 g (3.94 mmol, 56%).

TLC: DCM/MeOH 97:3, R_f **(2)** = 0.63.

^{1}H NMR (400 MHz, $CDCl_3$) δ = 5.85 – 5.73 (m, 6H, H-3, H-4, H-5, H-6, H-7, H-8), 5.60 (s, 1H, H-2), 3.70 (tr, *J* = 6.3 Hz, 2H, H-11), 2.14 (tr, *J* = 5.8 Hz, 2H, H-9), 1.68 (quint, *J* = 7.2 Hz, 2H, H-10) ppm.

Synthesis of the carboxylic acid derivate of cyclooctatetraene

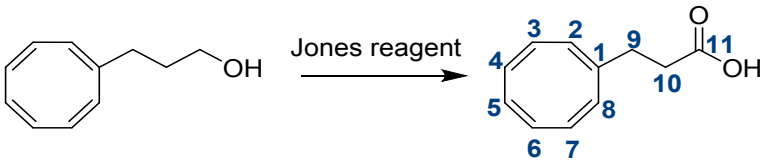

Cyclooctatetraenyl-propanoic acid (3): A solution of **2** (23.6 mg, 0.15 mmol) in 0.5 mL acetone and 100 µL Jones reagent (3 M) were stirred at 0 °C for 1 h. At this point, the reaction was quenched with MeOH and the solution was concentrated. The crude product was dissolved in EtOAc/H_2O and the water layer was extracted with EtOAc. Then, the combined organic phases were dried over Na_2SO_4 and concentrated to receive the crude acid as a yellowish oil. Yield: not determined.

TLC: DCM/MeOH 96:4, R_f (**3**) = 0.26.

^{1}H NMR (400 MHz, $CDCl_3$) δ = 5.90 – 5.69 (m, 6H, H-3, H-4, H-5, H-6, H-7, H-8), 5.62 (s, 1H, H-2), 2.49 (tr, *J* = 7.4 Hz, 2H, H-10), 2.40 - 2.32 (m, 2H, H-9) ppm.

Synthesis of the cyclooctatetraene NHS ester derivate COT-NHS

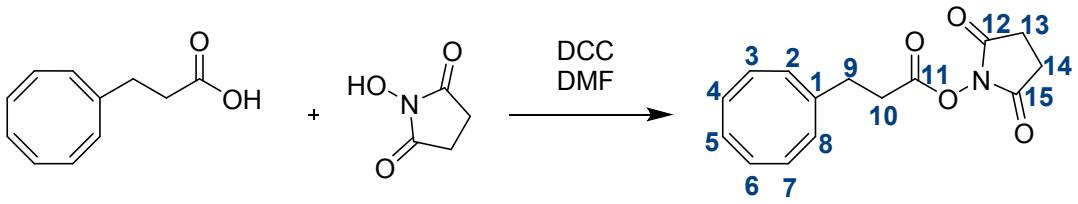

COT-NHS (4): To a solution of **3** (20 mg, 0.11 mmol) and *N*-hydroxysuccinimide (NHS) (32 mg, 0.28 mmol), in 1.5 mL DMF, *N,N´*-dicyclohexyl carbodiimide (DCC) (59 mg, 0.29 mmol) was added at 0 °C. The resulting mixture was stirred for 19 h at rt. Then, the reaction solution was concentrated and the crude product was purified by column chromatography (SiO_2, DCM/MeOH 19:1) to gain a light yellow oil. Yield: 8.2 mg (0.03 mmol, 26%).
TLC: DCM/MeOH 19:1, R_f **(4)** = 0.95.

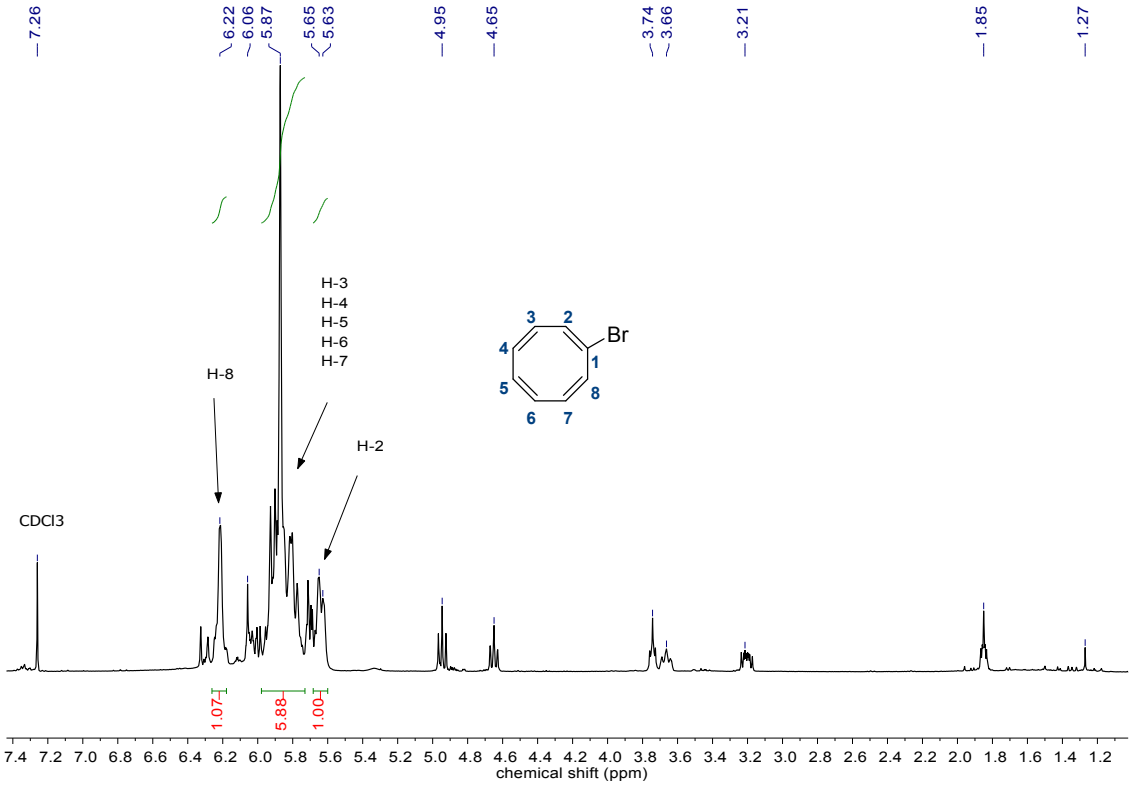

Figure S36: ^{1}H-NMR spectrum of brominated cylcooctatetraene 1.

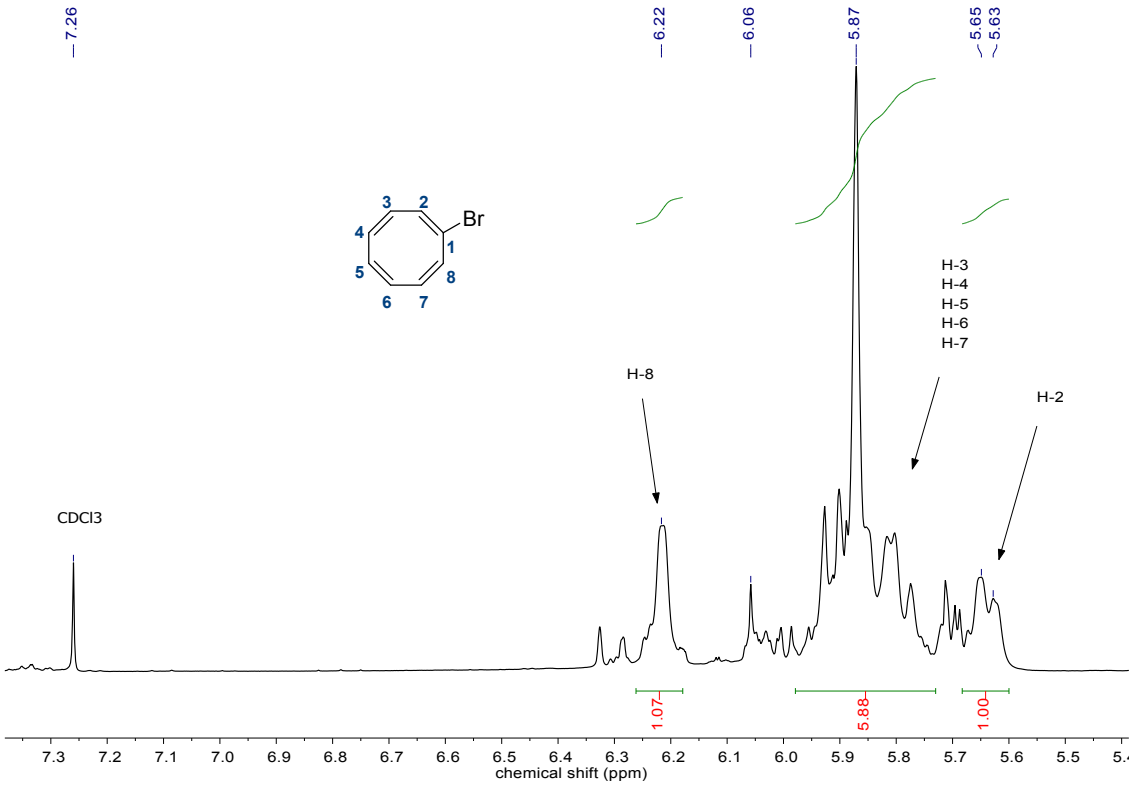

Figure S37: ^{1}H-NMR spectrum of brominated cylcooctatetraene 1 (7.35-5.42 ppm).

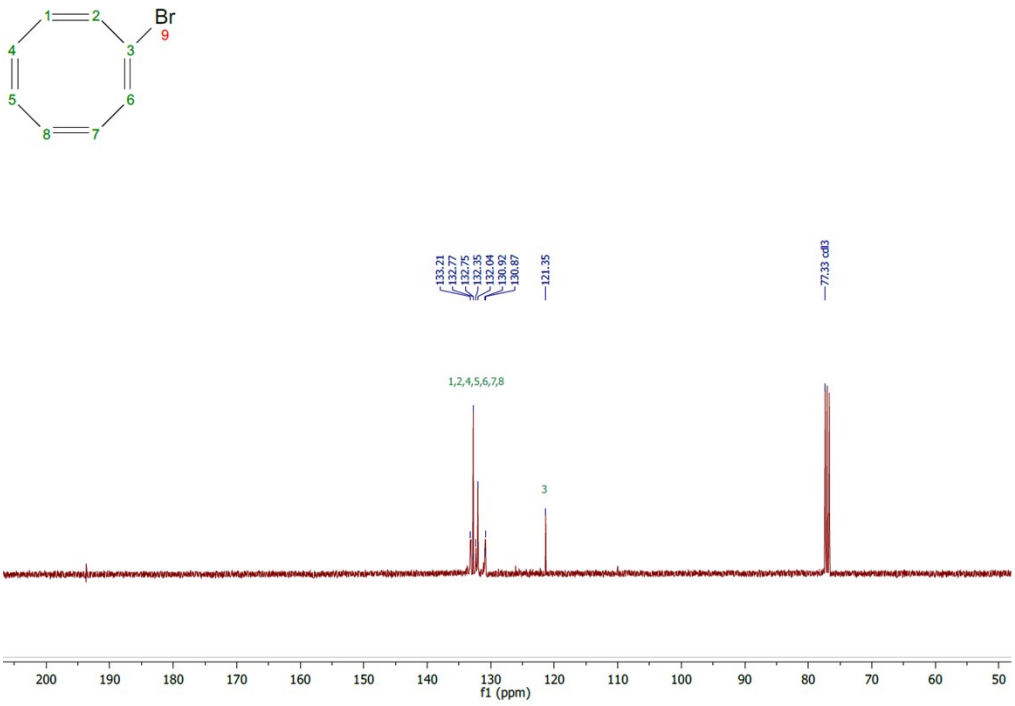

Figure S38: ^{13}C-NMR spectrum of bominated **cylcooctatetraene 1.**

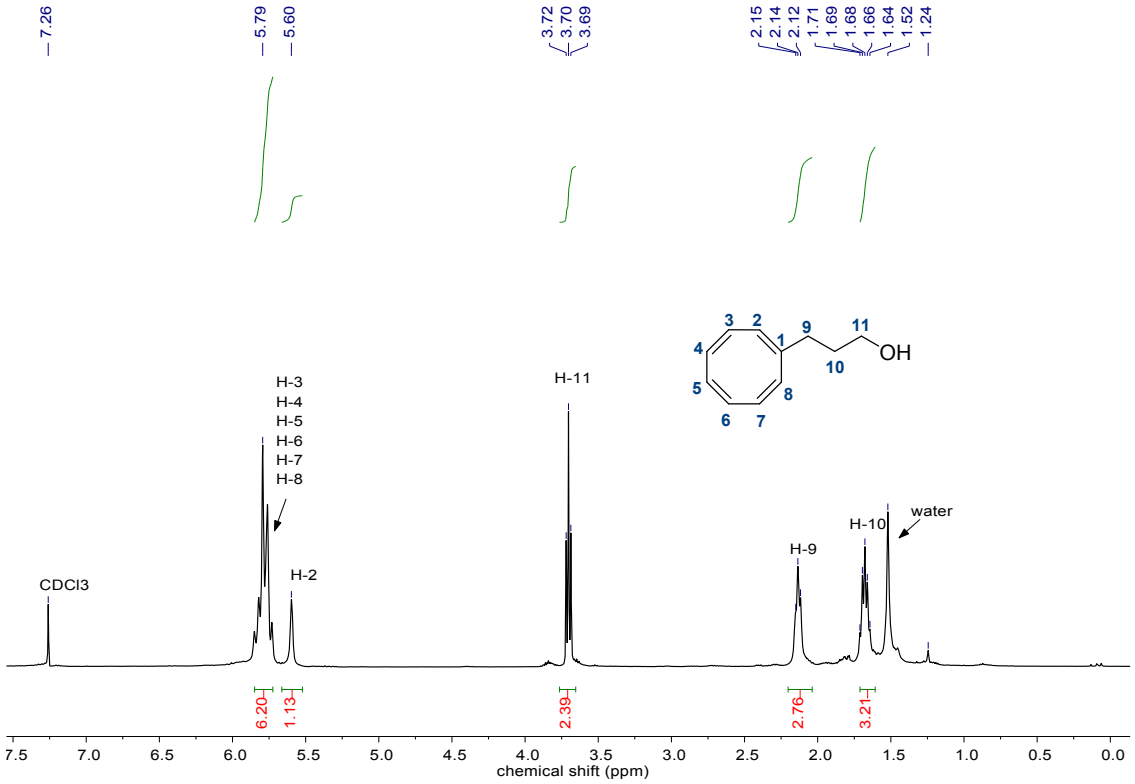

Figure S39: ^{1}H-NMR spectrum of alcohol 2.

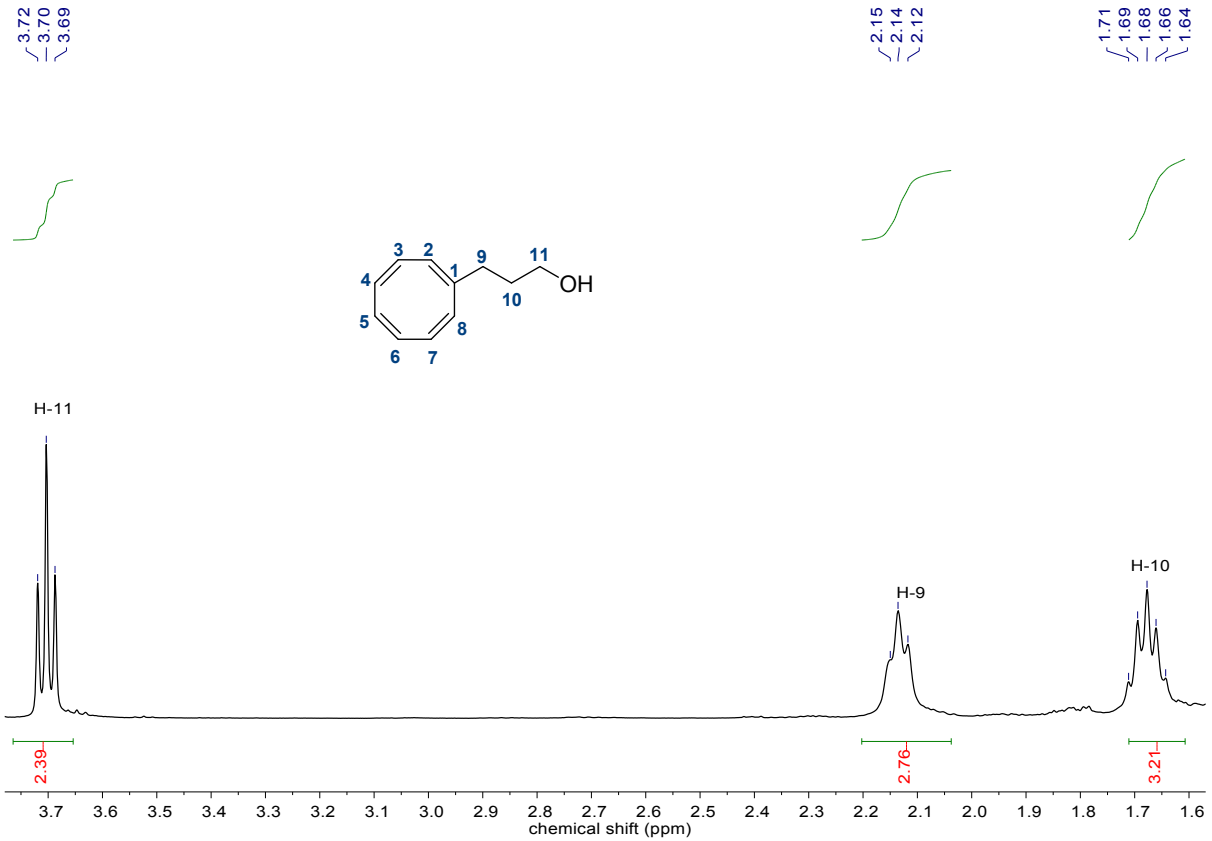

Figure S40: ^{1}H-NMR spectrum of alcohol **2** (3.78-1.57 ppm).

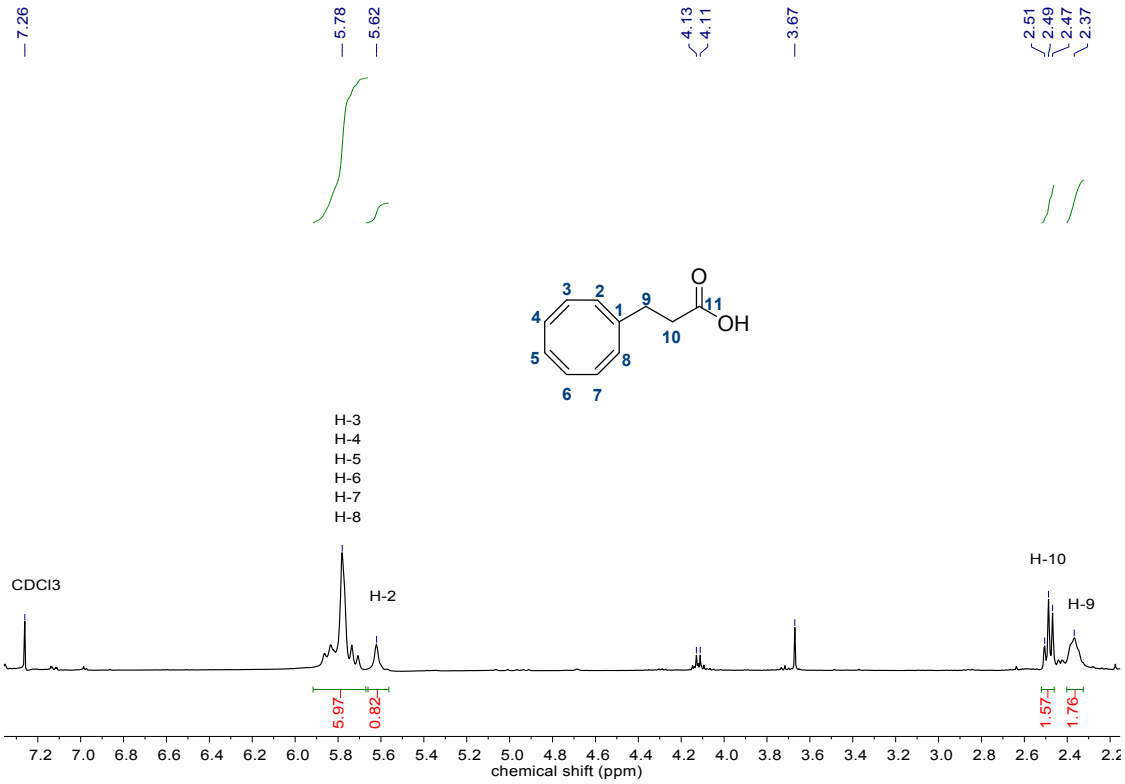

Figure S41: ^{1}H-NMR spectrum of acid 3.

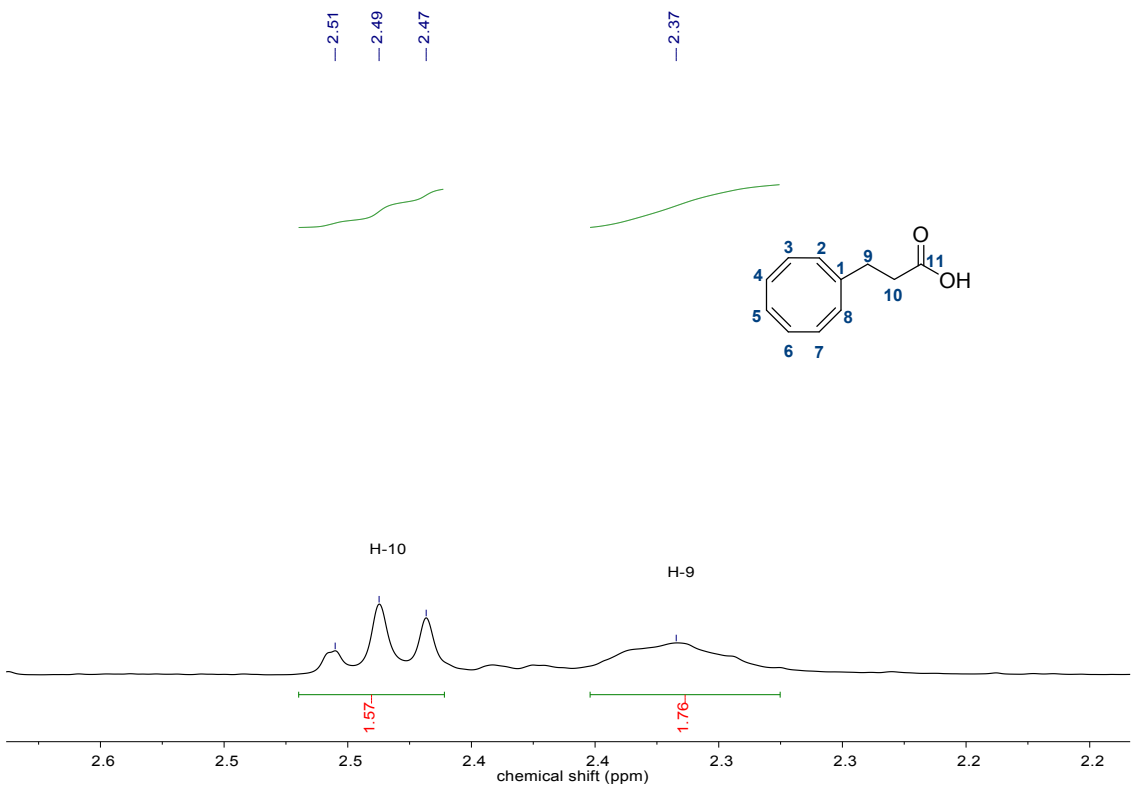

Figure S42: ^{1}H-NMR spectrum of acid **3** (2.86-2.12 ppm).

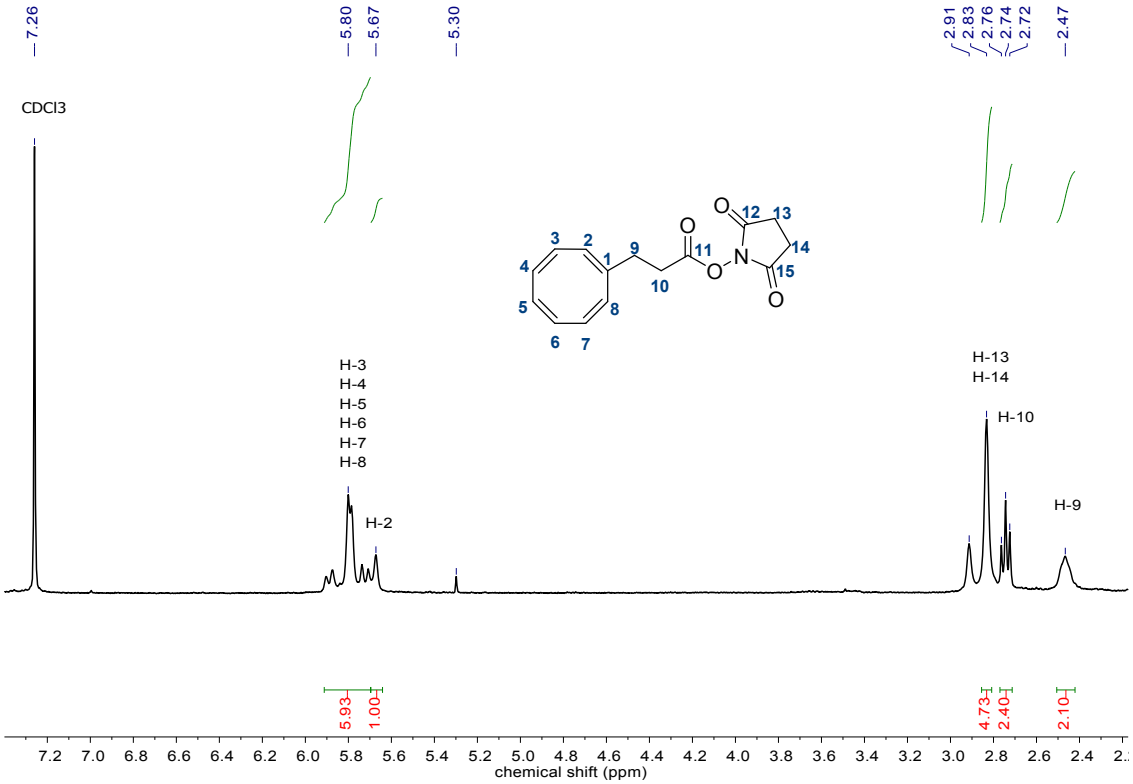

Figure S43: ^{1}H-NMR spectrum of reactive ester COT-NHS.

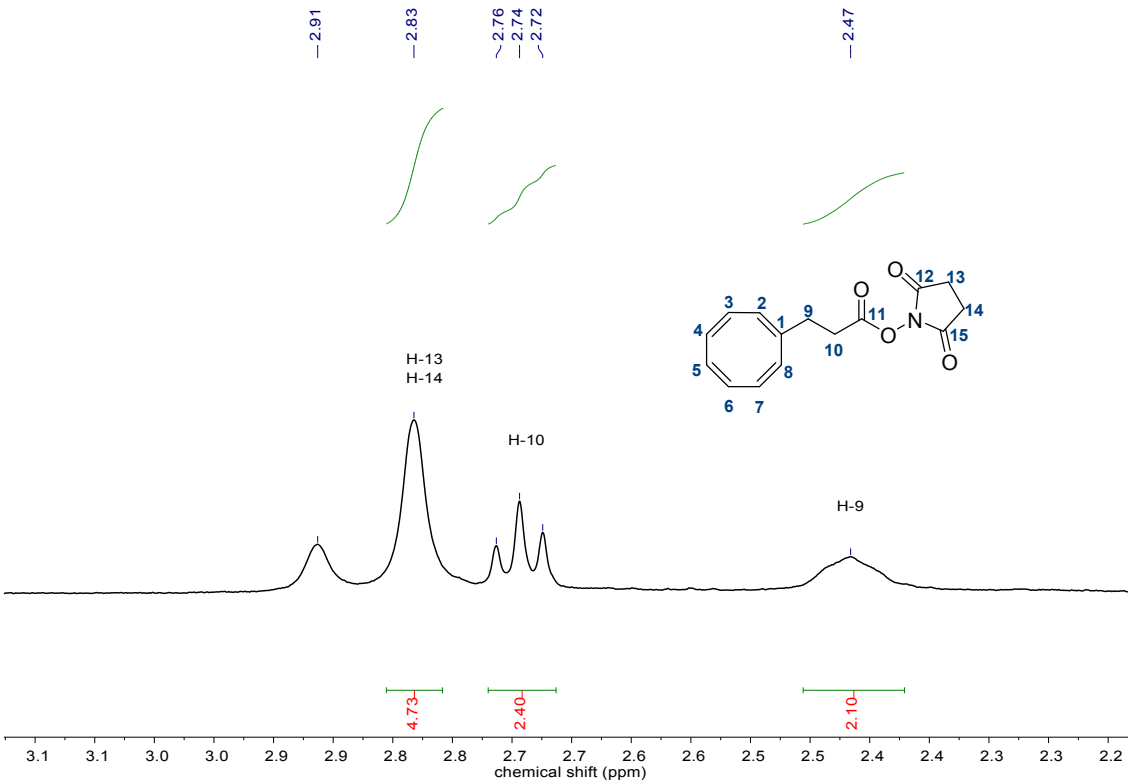

Figure S44: ^{1}H-NMR spectrum of reactive ester COT-NHS (3.22-2.16 ppm).

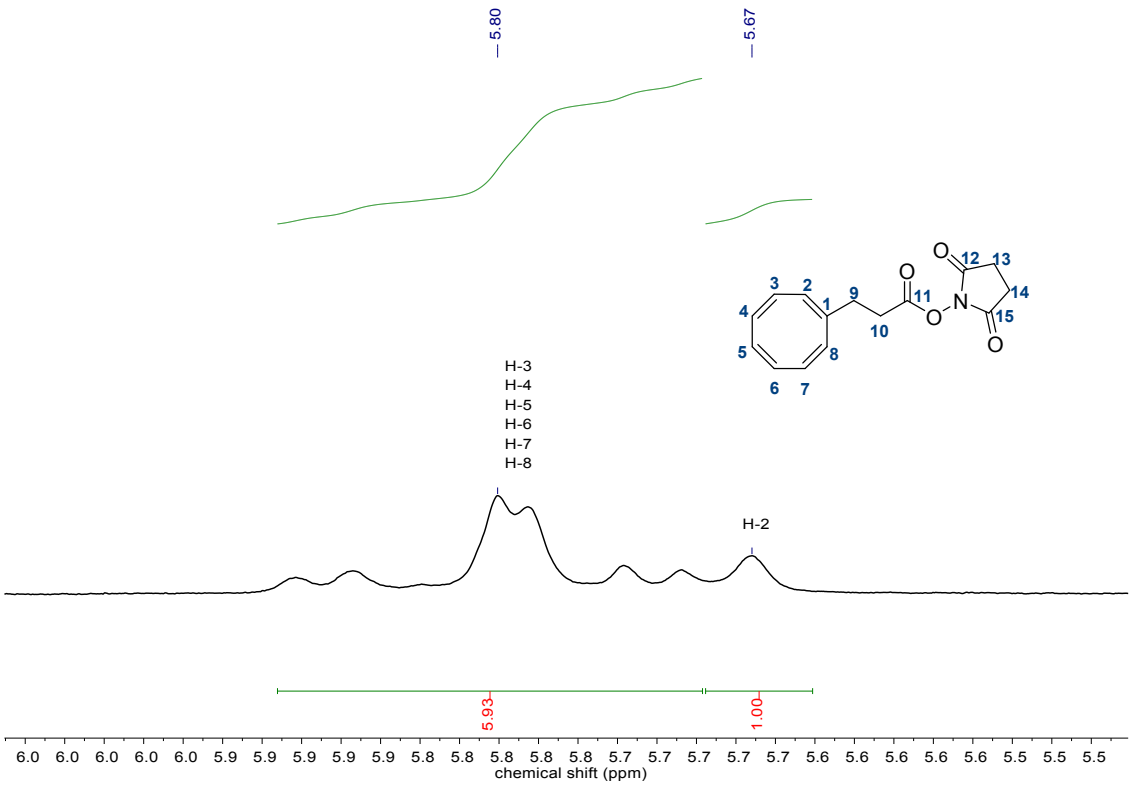

Figure S45: ^{1}H-NMR spectrum of reactive ester COT-NHS (6.05-5.49 ppm).

Synthesis of a DNA-COT conjugate

P2 COT*:* The lyophilized ssDNA-NH_2 named P2 (Biotin-5'-CGT CCA GAG GAA TCG AAT ATT A-3'-NH_2) was resuspended in MilliQ water and the concentration was adjusted to 20 µM in 0.2 M $NaHCO_3$ buffer (pH 8.35). To this solution, 50 equivalents of **COT-NHS** was added in 100 µL of DMF and the mixture was vortexed thoroughly. After incubation overnight, the oligonucleotide was purified on illustra NAP 5 column (*vide supra*) and isolated by preparative rp-HPLC (gradient 1, *vide supra*) to yield **P2-COT**. The yield was found to be 32% for coupling **COT-NHS** to ssDNA. MS (MALDI-TOF): 7537 g mol^{-1} (found), 7540 g mol^{-1} (calc.)

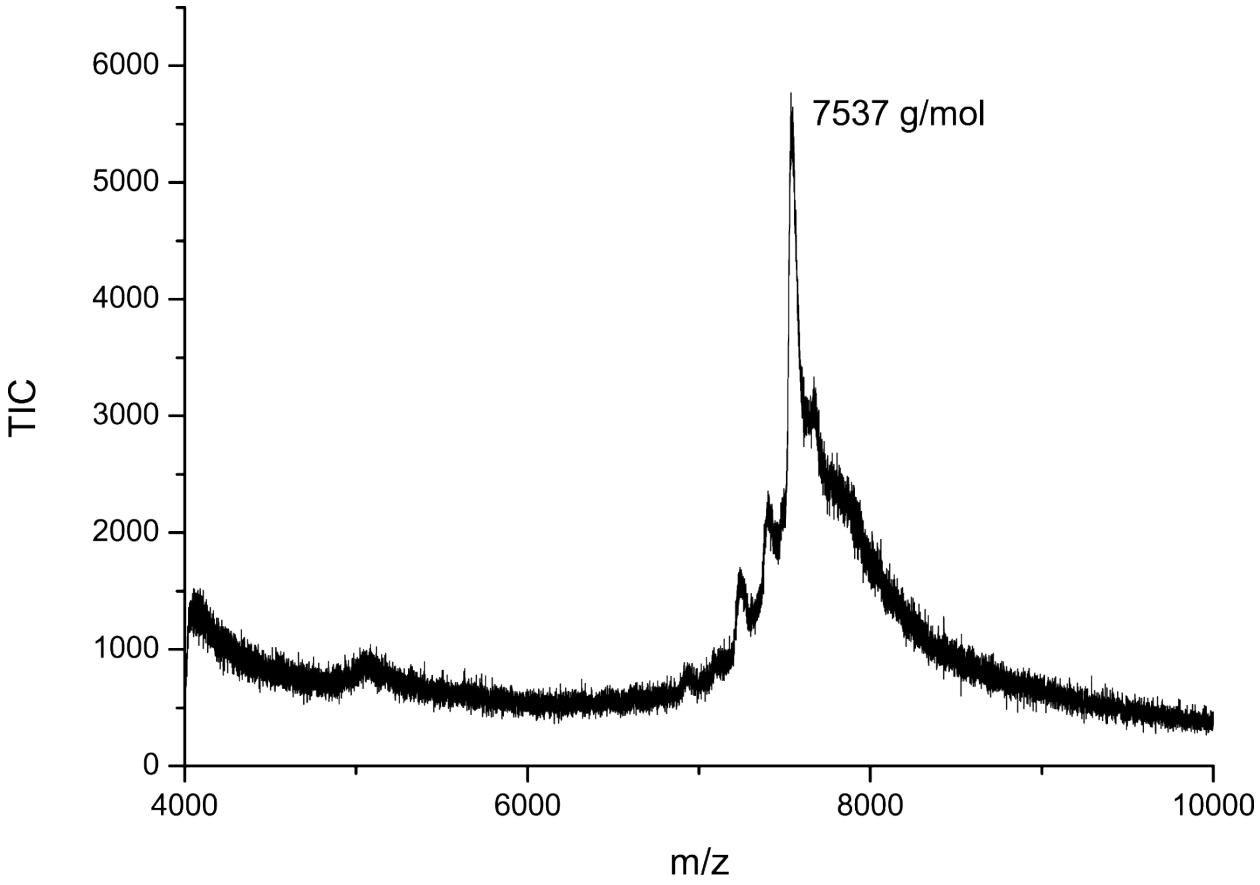

Figure S46: MALDI-TOF mass spectrum of P2-COT.

Characterization of DNA-Trp-fluorophore conjugates

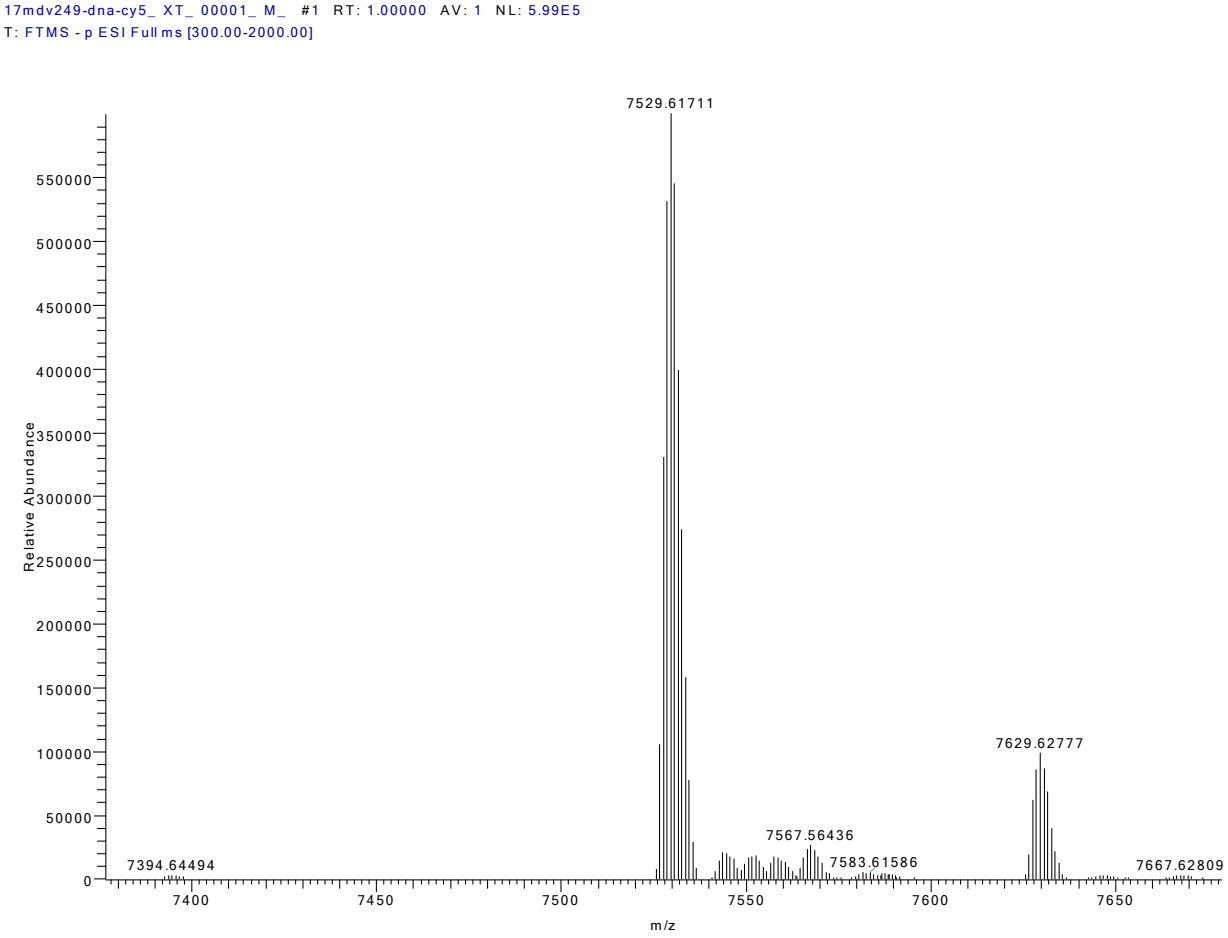

Figure S47: ESI-MS Spectrum of P1-Tryp-Cy5.

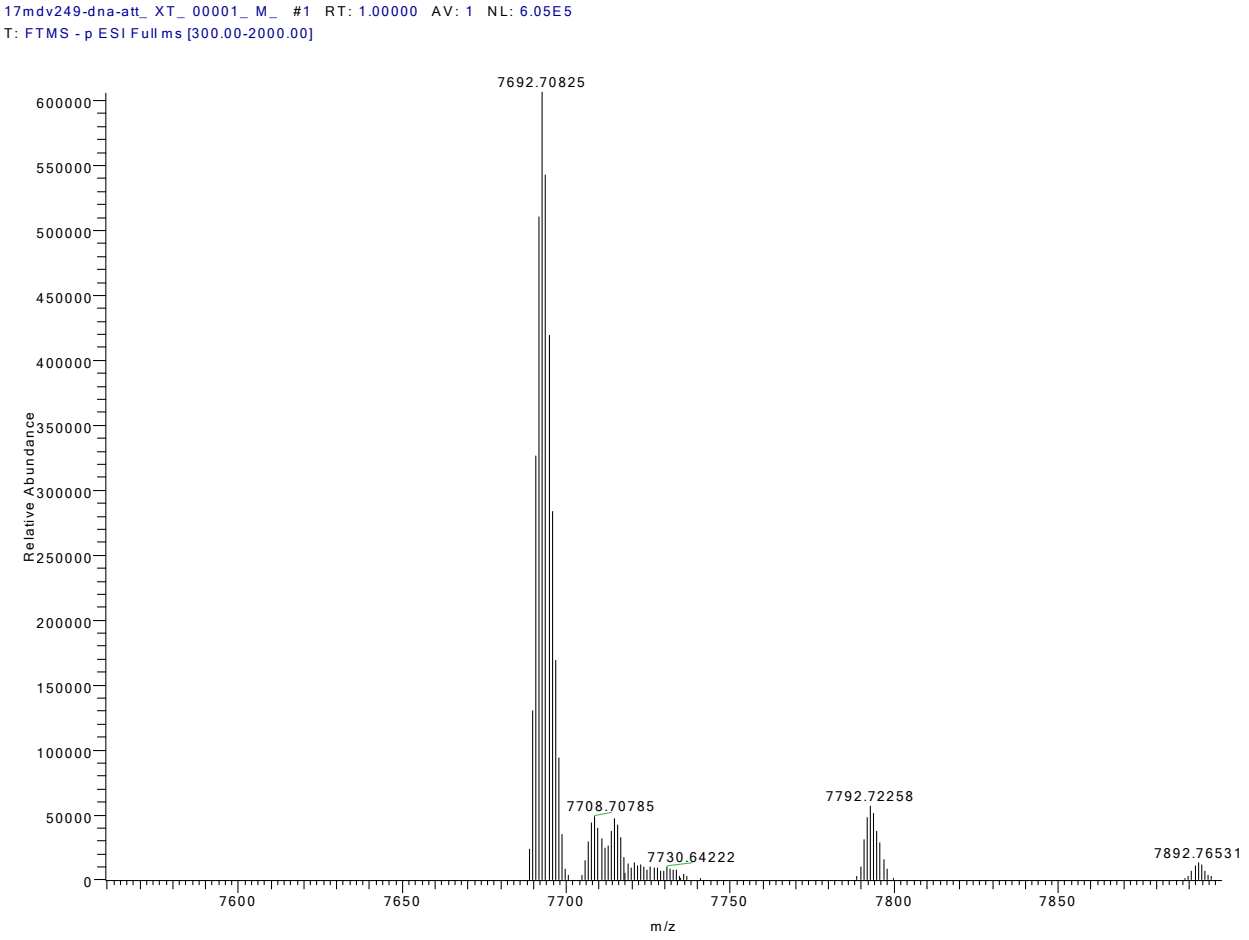

Figure S48: ESI-MS Spectrum of P1-Tryp-ATTO 647N.

3. References

(1) Altman, R. B.; Terry, D. S.; Zhou, Z.; Zheng, Q.; Geggier, P.; Kolster, R. A.; Zhao, Y.; Javitch, J. A.; Warren, J. D.; Blanchard, S. C. Cyanine Fluorophore Derivatives with Enhanced Photostability. *Nat. Methods* **2012**, *9* (1), 68–71.

(2) van der Velde, J. H. M.; Oelerich, J.; Huang, J.; Smit, J. H.; Aminian Jazi, A.; Galiani, S.; Kolmakov, K.; Guoridis, G.; Eggeling, C.; Herrmann, A.; et al. A Simple and Versatile Design Concept for Fluorophore Derivatives with Intramolecular Photostabilization. *Nat. Commun.* **2016**, *7*, 10144.